HHS Public Access

Author manuscript

ACS Infect Dis. Author manuscript; available in PMC 2019 July 13.

Published in final edited form as:

ACS Infect Dis. 2018 July 13; 4(7): 1130–1145. doi:10.1021/acsinfecdis.8b00090.

Small molecule inhibitors of metabolic enzymes repurposed as a new class of anthelmintics

Rahul Tyagi[1,#], **Amarendar Reddy Maddirala**[2,#], **Mostafa Elfawal**[3,#], **Chelsea Fischer**[4], **Christina A. Bulman**[4], **Bruce A. Rosa**[1], **Xin Gao**[1], **Ryan Chugani**[2], **Mingzhou Zhou**[2], **Jon Helander**[2], **Paul J. Brindley**[6], **Chih-Chung Tseng**[7], **Iain R. Greig**[7], **Judy Sakanari**[4], **Scott A. Wildman**[5], **Raffi Aroian**[3,*], **James W. Janetka**[2,*], and **Makedonka Mitreva**[1,8,*]

[1]McDonnell Genome Institute, Washington University School of Medicine, 4444 Forest Park Ave, St. Louis, Missouri 63108, USA

[2]Department of Biochemistry and Molecular Biophysics, Washington University School of Medicine, 660 S. Euclid Ave., Box 8231, St. Louis, Missouri 63110, USA

[3]University of Massachusetts Medical School, Suite 219 Biotech 2, 373 Plantation St., Worcester, Massachusetts 01605, USA

[4]Department of Pharmaceutical Chemistry, University of California San Francisco, 1700 4th St, San Francisco, California 94158, USA

[5]UW Carbone Cancer Center, School of Medicine and Public Health, University of Wisconsin-Madison, 1111 Highland Ave., Madison, Wisconsin 53792, USA

[6]Department of Microbiology, Immunology & Tropical Medicine, and Research Center for Neglected Diseases of Poverty, School of Medicine and Health Sciences, George Washington University, Ross Hall, Room 521, 2300 Eye Street, NW, Washington, DC 20037, USA

[*]Corresponding authors : Raffi.Aroian@umassmed.edu (RA); janetkaj@wustl.edu (JJ); mmitreva@wustl.edu (MM).
[#]Equal contribution
ORCID
Makedonka Mitreva: 0000-0001-9572-3436

AUTHOR CONTRIBUTIONS

M.M. J.W.J., P.J.B., and R.A., conceived and designed the experiments. RT, J.J., and MM wrote the manuscript. A.R.M, R.C., and J.H, synthesized the compounds. C.F., C.A.B, J.S., M.E., performed in vitro and in vivo screening. M.Z., and J.H., performed the bioaccumulation assay. M.E, and C.A.B., prepared samples for the bioaccumulation assays. R.T., X.G., B.A.R., S.A.W., analyzed all the data. All authors edited the manuscript.

The authors declare no competing financial interest.

ASSOCIATED CONTENT

Supporting Information

Figures S1–S45. Detailed information related to compound spectral data, general method and procedures, 1H-NMR & LCMS spectral data for compounds **6(a–o)**, **10(a–b)**, **17(a–b)**, **23(a–c)** & **24(a–c)** (Figure S1–S26). Time- and species-dependence of the IC_{50} values (Figure S27). Bioaccumulation assay data (Figure S28–S44). RNAseq based gene expression profiles (Figure S45). (PDF)

Tables S1–S6. Table S1. CPT orthologs based on orthoMCL of 16 nematode species, seven host species and two outgroups. Table S2. ChEMBL compounds linked to orthologous targets of nematode CPTs. Table S3. Selected available representatives drug-like compounds for screening in parasitic nematodes. Table S4. Results of the *in vitro* screening of various concentrations of the commercially available and synthesized compounds on multiple species of nematodes. Table S5. Amino acid variances in the nematode CPT2 sequences docking pocket (inferred based on the homology models). Number of amino acids diverse between reference (Rat CPT2; PDB id: 2FW3) and parasite CPT2 homolog within 5 and 10 Angstroms of the binding pocket. Table S6. Summary results of the bioaccumulation assay (all bioaccumulation analysis figures are available as Figure S28–S44). (XLSX)

[7]Kosterlitz Centre for Therapeutics, University of Aberdeen, Foresterhill, Aberdeen, AB25 2ZD, U.K.

[8]Division of Infectious Diseases, Department of Medicine, Washington University School of Medicine, 4523 Clayton Ave., CB 8051, St. Louis MO, 63110, USA

Abstract

The enormous prevalence of infections caused by parasitic nematodes worldwide, coupled to the rapid emergence of their resistance to commonly used anthelmintic drugs, presents an urgent need for the discovery of new drugs. Herein, we have identified several classes of small molecules with broad spectrum activity against these pathogens. Previously, we reported the identification of carnitine palmitoyltransferases (CPTs) as a representative class of enzymes as potential targets for metabolic chokepoint intervention that was elucidated from a combination of chemogenomic screening and experimental testing in nematodes. Expanding on these previous findings, we have discovered that several chemical classes of known small molecule inhibitors of mammalian CPTs have potent activity as anthelmintics. Cross-clade efficacy against a broad spectrum of adult parasitic nematodes was demonstrated for multiple compounds from different series. Several analogs of these initial hit compounds were designed and synthesized. The compounds we report represent a good starting point for further lead identification and optimization for development of new anthelmintic drugs with broad spectrum activity and a novel mechanism of action.

For Table of Contents Use Only

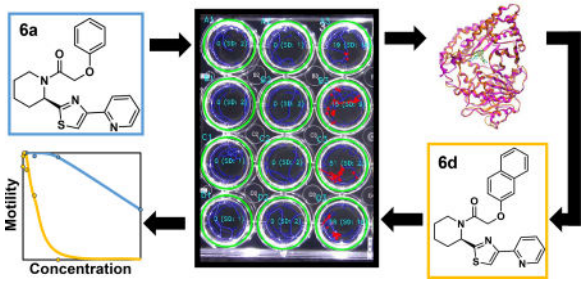

Keywords

Parasitic nematodes; hookworm; whipworm; filarial nematode; whole worm assay; in vitro; in vivo; target class repurposing; Carnitine palmitoyltransferase (CPT); bioaccumulation; anthelmintic

Parasitic nematodes (roundworms) are the causative agents responsible for multiple infectious diseases affecting over 2 billion people[1], as well as contributing to loss of 10% of cultivated crops[2] and substantially reducing production of meat, milk and wool in domestic livestock[3] worldwide. Although not commonly fatal in humans, these diseases significantly contribute to an enormous economic burden associated with lost productivity and perpetuation of poverty cycle (>3 million years lived with disabilities (YLDs)) as well as imposing a heavy burden on associated healthcare costs. Indeed, they are among the most prevalent of parasitic diseases worldwide. The combination of the global healthcare burden,

their prevalence, and lack of effective treatment options have led to their inclusion in the World Health Organization's (WHO) list of neglected tropical diseases.[4]

Mass drug administration (MDA) programs over the last two decades have led to a significantly reduced prevalence of some, but not all, of these diseases. Unfortunately, these efforts use only a small number of antiparasitic drug classes[5], mostly benzimidazoles (e.g. albendazole), targeting tubulin in nematodes (intestinal infections) and macrocyclic lactones (e.g. ivermectin) targeting chloride ion channels, and used in combination with diethylcarbamazine (an inhibitor of arachidonic acid metabolism) for filarial MDAs[6–7]. Importantly, the large scale usage of these drugs has led to wide-spread resistance in parasitic nematodes of farm animals and concerns of similar resistance either crossing over or independently emerging in human parasites, which may already be occurring.[8] In recent years, a limited number of new drugs with diverse mechanisms of action have been championed. These include the nicotinic receptor agonists (tribendimidine) or antagonists (monepantel)[9] as well as a drug that has been proposed to target the protein kinase C signaling cascade (emodepside)[10]. However, none of these newly identified drugs are yet approved for use in humans, and resistance may quickly evolve against them, as shown for monepantel against the barber's pole worm *Haemonchus contortus*.[11] Therefore, there is a pressing need to develop novel small molecule anthelmintics encompassing new modes of actions.

One strategic opportunity to identify an entirely novel class of anthelmintic(s) is to target metabolic pathways essential to the viability of the parasites[12–13]. Given the accelerated pace and increased availability of genome scale information related to parasitic nematodes, it is possible to perform pan-phylum comparative analyses of genes and pathways involved, for example, with metabolism.[13] These pan-phylum analyses have the potential to identify novel targets of essential metabolism and to guide the development of drugs with new modes of action with broad applicability across the diverse clades of the phylum Nematoda. This is desirable since co-infections with multiple parasitic species routinely occur, and economics disfavor the development of drugs for individual parasites. Previously, knowledge-based targeting of metabolic networks for pathogens has been used to identify novel candidates for drugs.[14] Specifically, enzymes that either uniquely consume or produce a metabolite (termed "chokepoint" enzymes) have been targeted; inhibition of chokepoint activity is expected to be deleterious due to the absence of alternative pathways to compensate for their function. Similar approach at a much smaller scale has been applied to nematodes by this group[12] where putative chokepoints in multiple species of worms were identified and a prioritization of both the individual chokepoint enzymes and their associated inhibitors in drug-target databases was performed.

The carnitine palmitoyltransferase (CPT) family of enzymes (EC 2.3.1.21) is a chokepoint in nematodes. CPTs are mitochondrial membrane-embedded enzymes that participate in transport of long chain fatty acids from the cytoplasm to the internal matrix of the mitochondrion, where they can be oxidized to release energy. Several classes of small molecule inhibitors have been described as CPTs were promising targets for type 2 diabetes and insulin resistance for many years[15–16]. Available chemical classes of inhibitors include oxirane carboxylic acids, which are irreversible covalent inhibitors and acylcarnitine analogs

which are substrate competitive inhibitors.[15] Further, homologous enzymes in humans have been reported to be targeted by perhexiline (PHX),[15] a marketed drug indicated for treatment of angina pectoris and ischemic heart disease.[17] In our previous work, we showed PHX to be effective against the early larval stages of *Caenorhabditis elegans*, the blood-feeding parasitic nematode *H. contortus*, and the filarial nematode *Onchocerca lienalis*.[12] However, efficacy against adult parasites, which are the targets of chemotherapy, had not yet been shown.

To expand on our initial findings, we undertook a target class repurposing[18] approach and tested known drug-like small molecule CPT inhibitors of the mammalian enzymes CPT1A, 1B and CPT2. To this end, we first purchased several compounds known to be CPT inhibitors and then synthesized representative examples of three other classes of heterocyclic CPT inhibitors that were not commercially available. Next, we developed a homology model of the nematode enzyme CPT2 and rationally designed analogs with modifications to selectively target nematode CPT2 over mammalian CPT2. We have systematically studied gene sequence variations (*e.g.*, indels) among nematodes and hosts, where we identified variants specific to the phylum Nematoda. We subsequently characterized their structural impact on the variant proteins and then proposed their relevance to selective anthelmintic drug targeting.[19] These compounds were synthesized and tested *in vitro* for their efficacy using phenotypic whole worm assays with a broad variety of nematode species having diverse modes of parasitism, including hookworms and whipworms, which reside within the lumen of the intestine, as well as filariids which live within the blood and solid tissues. PHX was further tested in an *in vivo* assay using hamsters infected with the intestinal zoonotic hookworm parasite, *Ancylostoma ceylanicum*.

RESULTS AND DISCUSSION

Hit identification of initial compounds for targeting nematodes

Two orthogonal approaches, both based on an underlying target class repurposing strategy, were followed to identify potential anthelmintics, based on existing mammalian CPT inhibitors. First, chemogenomic screening was performed to locate CPT homologs (Table S1) among the target proteins in the ChEMBL database using sequence similarity. This process identified 105 candidate compounds (Table S2), including PHX (**P1** in Figure 1A) which has been reported to be active against the free living nematode *C. elegans* as well as larval stages of intestinal and filarial nematode parasites.[12] **P1** is a clinically used antianginal agent that weakly inhibits both CPT1 and CPT2 in humans,[15] as well as other targets including certain Ca^{2+} and K^{+} channels.[20] A subset of these 105 compounds was selected by structural diversity, employing a stepwise scheme of prioritization. First, the compounds were clustered based on their fingerprint Tanimoto similarity scores[21] and subsequently, compounds were rejected based on undesired physical properties[22], lack of commercial availability, and cost.[23] This filtering strategy resulted in the identification of nine compounds for testing in a whole organism phenotypic screen, of which five (**P1–P5**) were initially selected for screening (Figure 1A and Table S3).

In a parallel second approach, four known small molecule inhibitors of mammalian CPT1A, 1B and CPT2[15] were synthesized (Schemes 1 and 2). These are compounds **6a**, **10a**, **17a**,

and **17b**. **6a** and **10a** belong to the phenoxyacetamide piperidinyl, and bis-phenylsulfonamide acid series of inhibitors, respectively. **17a** and **17b** (Scheme 2) are conformationally restricted analogs of the latter series which cyclize the sulfonamide into a fused ring. **6a** is known to target rat and human CPT1A potently and selectively over CPT1B with some activity for CPT2. In contrast, **10a** is less active for CPT1A and shows some activity for CPT1B and CPT2. **17a** is 10-fold more potent inhibitor of CPT1A relative to **10a** and is totally selective over CPT1B, like **6a**. **17b** is similar to **10a** since it has less CPT1A potency and is the most active against CPT1B. Of all compounds, **17a** is the most active against CPT2. These compounds were chosen for synthesis and biological evaluation because they belong to four different chemical series in addition to their different selectivity profiles for the CPT isoforms.

Compound screening with parasitic nematodes in a phenotypic motility assay

The resulting nine compounds that we identified and prioritized were experimentally screened with five diverse species of parasitic nematodes that broadly span the phylum Nematoda by including representatives from three nematode clades[24] (Figure 2): Clade I (whipworm *Trichuris muris*), Clade III (filarial *Brugia pahangi*) and clade V (strongylids *Ancylostoma ceylanicum*, *Nippostrongylus brasiliensis* and *Heligmosomoides polygyrus*). For these tests, the adult developmental life cycle stages of each species were assayed. The adult stage of the worm generally represents the most relevant form for assessing their susceptibility to anthelmintic therapy and can display different responses from those of worms at the larval stages. This is particularly relevant for compounds that target metabolism, which can vary substantially during the developmental cycle of the nematode[13]. For example, larval stages of some soil transmitted helminths (STHs), such as hookworms, live in the soil, whereas the adult forms parasitize the GI tract of the mammalian host. These assays also included known anthelmintics as positive controls (pyrantel for hookworm and levamisole for whipworm) and a negative control (DMSO).

Three of the five compounds from the first set of candidate inhibitors (**P1**, **P2**, **P5**) showed deleterious effects on one or more parasitic species (Figure 2). It was gratifying to find that **P1** (PHX) showed good potency against the worms but it is very structurally distinct from other known CPT modulators[15]. Whereas it has long been thought that antianginal activity of PHX may be a direct consequence of its inhibition of CPT2 (or other unknown) activity, resulting in the fuel switch from fatty acid to glucose in the heart, PHX may cause more complex metabolic changes.[25] **P2** showed selective activity against *T. muris* (whipworms)[15, 26–27] while **P5** showed broad anthelmintic activity against both *A. ceylanicum* (hookworms) and whipworms.[15] Of the synthesized analogs, **6a** and **10a** showed significant pan-nematode effects by decreasing the motility of the worms in more than one species. Finally, compound **17a** showed some activity against hookworms and the filarial species *B. pahangi*.

In summary, we found that six of the nine compounds tested were deleterious for one or more of the parasitic species (Table S4), and three of the six (**P1**, **6a**, **10a**) displayed pan-nematode effects (inhibiting at least one intestinal and a filarial species). **P1** and **6a** displayed the best pan-nematode effects in the whole worm assay by inhibiting multiple

intestinal and filarial species and **10a** was efficacious in only one intestinal species and a filarial species (Figure 2 and Table S4).

Expanding the list of small molecules with pan-phylum inhibition potential

To expand on the structure activity relationships (SAR) of our hit compounds with the best pan-phylum inhibitory effect, we searched for available analogs. PHX is used in the clinic only in Australia, and New Zealand, but not elsewhere because of hepatic toxicity and peripheral neuropathy in patients with impaired metabolism resulting from polymorphism in the cytochrome P-450 enzyme (CYP2D6) which leads to high plasma concentrations of the drug.[20] Recent findings revealed improved pharmacokinetic (PK) properties of synthetic fluorinated analogs of PHX.[28] Thus, we acquired two of the PHX analogs (cycloalkyl analog **P1a** and fluorinated analog **P1b**)[28] and experimentally screened them against a whipworm and a filariid nematode (Table S3 and Table S4). **P1a** significantly reduced activity in both the whipworm (60 μM at 24 and 48 hrs) and filarial worm (inhibition of worm motility of 99% with 75 μM and 175 μM within the first 24 hrs, day 0). Compound **P1b** completely inhibited the whipworm's motility after 48 hrs with 60 μM and was similar to **P1a** in inhibiting filarial worm motility. While these analogs have improved pharmacokinetic properties, there was no effect on their anthelmintic activity relative to PHX.

In order to further understand our results from the phenotypic screening of the worms, we used compounds **6a** and **10a** to derive initial SAR (Figure 1B) through molecular modeling studies. As illustrated in Figure 3, we built a series of CPT2 homology models using an inhibitor-bound *Rattus norvegicus* (rat) X-ray crystal structure (PDB code: **2FW3**), for four nematode species (*T. muris, A. ceylanicum, C. elegans, Strongyloides stercoralis*) and three mammalian hosts (*Mus musculus, Mesocricetus auratus, Homo sapiens*). Thereafter, we performed molecular docking studies using **6a**, **10a**, **17a**, and **P1** (Figure 3B). We employed multiple parasitic nematode species for this analysis because CPT2 is conserved among nematodes, all orthologs of which are divergent from the mammalian ortholog (Table S5).

Based on this analysis derived from SAR and the molecular modeling studies, we rationally designed focused libraries based on **6a** and **10a** (Figure 4). Two modifications to **6a** having the most productive effect were derivatives of the phenyl ether portion (Scheme 1A). Two additional analogs, **6n** and **6o** were designed based on the overlay of **6a** with **10a** and **17a** (Figure 3B), both of which contain a phenyl carboxylic acid that makes an electrostatic interaction with the conserved histidine residue in human (His372), His571 in hookworm and His380 in whipworm. This was absent in **6a** and was predicted to improve the binding affinity to CPT2 and improve potency in the motility assay. The methyl ester intermediates **6l** and **6m** were also tested for their activity. It was predicted that the methyl esters would increase permeability to the worms, acting as prodrugs and would hydrolyze into the predicted active carboxylic acid prior to engaging CPT1 or 2 in the mitochondrial membrane of the nematode cell. For **10a**, we pursued changing the sulfonamide to a urea with three analogs **24a–c** (Scheme 3) and also tested the methyl ester derivatives **23a–c** as prodrugs of the carboxylic acid once again to assess differential effects in penetration of the nematode cuticle.

Synthesis of compounds

The synthesis of the small molecule inhibitors **6(a–k)** are outlined in Scheme 1A (Figure S1–S15). Reaction of compound **1** acid with ammonium chloride in presence of base yielding amide **2**, which is converted to thioamide **3** by treating with Lawesson's reagent. The heterocyclic thiazole compound **4** were prepared by refluxing of compound **3** with appropriate 2-bromo (5-substituted pyridine)-1-one and $CaCO_3$, which upon Boc-deprotection of intermediate **4** followed by coupling of appropriate acid yields **6(a–k)**. Compounds **10(a–c)** were synthesized according to Scheme 1B (Figure S16–S18), where reaction of commercially available methyl-3-amino benzoate **8** with an appropriate 3,4–substituted benzene sulfonyl chloride **7(a–c)** in the presence of base, followed by ester hydrolysis yielded compounds **9(a–c)**. In turn, these intermediates were coupled with methyl-4-amino benzoate using standard amide bond coupling reagents EDCI/DIPEA/DMF. Subsequent hydrolysis of compounds **9(a–c)** yielded the final target compounds **10(a–c)**.

The synthesis of inhibitors **17(a–b)** is outlined in Scheme 2 (Figure S19–S20). Condensation of compounds **11**(**a–b**) with aryl sulfonyl chlorides **12**(**a–b**) in presence of base (pyridine) yields sulfonamide intermediates **13**(**a–b**). The methyl esters were converted to the carboxylic acids **14**(**a–b**) by basic hydrolysis, followed by coupling with amines **15** (**a–b**) using EDC/DIPEA/DMF. The resulting amides **16**(**a–b**) were hydrolyzed to provide the final targets **17**(**a–b**). Compounds **24(a–c)** are functionally distinct analogs of compounds **10**(**a–c**) in which the sulfonamide group is replaced by a urea. These were synthesized (Scheme 3; Figure S21–S26) by coupling of amine **18** with 3-nitro benzoyl chloride **19** which furnished intermediate **20**. Next, sequential catalytic reduction of both protecting groups yielded aniline **21**. Installation of the urea group was accomplished via reaction with isocyanates **22(a–c)** giving intermediate esters **23**(**a–c**), which were hydrolyzed to give the carboxylic acids **24(a–c)**.

Biological evaluation of rationally designed nematode inhibitors

We tested the new analogs for broad spectrum potential by screening three species spanning the phylum (Table S5): two intestinal parasites (Clade V – *A. ceylanicum* and Clade I – *T. muris*) and a filarial parasite (Clade III – *B. pahangi*). Three of the 10 analogs of **6a** (**6c**, **d, j**) were effective against *T. muris* and *B. pahangi* whereas **23a–c** and **24a–c** (analogs of **10a**) had only a species-specific effect with efficacy against the filarial nematode, *B. pahangi*. In addition, as evidenced by the IC_{50} values, two analogs (**6c, d**) were much more potent compared to **6a** (Table S4) against both *B. pahangi* (14 and 11 vs. 96 μM) and *T. muris* (118 and 32 vs. 195 μM). Time- and species-dependent IC_{50} values are provided in Figure S27.

The compounds **6l–o** were designed (Figures 3 and 4) to incorporate a carboxylic acid, as observed from docking analyses to make an electrostatic or H-bonding interaction with His372 of CPT2 like that of the benzoic acid of **10a, 17a and 17b**. In addition to the carboxylic acids (**6n** and **6o**), the methyl esters (**6l** and **6m**) were prepared as prodrugs thought to increase penetration of the worm outer cuticle. Interestingly, only the methyl esters **6l** and **6m** showed any noticeable activity, with the most active of the four, **6m**, requiring 250 μM and 175 μM concentrations to inhibit motility for *T. muris* and *B. pahangi*,

respectively, at 48 hours. The free acids had negligible activity on either *B. pahangi* or *T. muris* (Table S4), possibly indicating poor cuticle permeability.

Differential activity is potentially related to worm cuticle membrane penetration and uptake

One possible explanation for the differential phenotypic activity of the compounds tested among intestinal species may be differential penetration of the cuticle between species. Bioaccumulation assays (Figure S28–44) of **P1**, **6a** and **10a** by LC-MS of lysates of *T. muris* after incubation with these compounds clearly detected **P1** and **6a** using the 210 nm channel and MS identification of the parent compound, but not **10a** (Table S6 and Figure S28–S44). This would support that activity in *T. muris* results from this differential uptake of these compounds into the worm.

In *B. pahangi*, neither compound **6a** nor **10a** was observed at the incubation concentrations used, both having IC_{50} values less than 100 μM; however, **6f**, which has negligible activity, was present in high quantities. P1 (and analogs **P1a** and **P1b**) was observed; however, it was observed near the limit of detection, likely due to low concentrations used and weak recovery. The pro-drug compounds **6l** and **6m** were observed in much higher abundance than their free-acid counterparts **6n** and **6o**, respectively, supporting the hypothesis that uptake into the cuticle may benefit by increasing hydrophobicity of the compounds.

In vivo activity of Perhexiline in hookworm-infected hamsters

To ascertain whether our newly discovered class of pan-nematode chokepoint inhibitors possessed therapeutic utility in parasitic nematodes, Syrian hamsters (*Mesocricetus auratus*) infected with *A. ceylanicum* were treated with PHX (**P1**) at 100 mg/kg *per os*. Although the treatment had no marked effect on the worm load, there was a significant reduction in *A. ceylanicum* eggs/gram of feces compared to untreated control (Figure 5A and B). This result suggested that the target of **P1** (either a CPT isoform or another target) may interfere with reproduction in hookworms at the concentration resulting from this treatment or that generalized intoxication of the parasites *in vivo* led to a reduction in reproduction. Pertinent and consistent with the former, metabolic enzymes like CPT are essential for oocyte development in mammals,[29] and beta-oxidation plays a critical role in egg production in schistosomes, a flatworm parasite of mammals.[30] The observation that **P1** causes significant impaired egg production is supported by the RNAseq based developmental gene expression profiles of CPTs in *A. ceylanicum* which shows lower expression of CPT1/2 in L4 female compared to adult female and compared to L4 male and adult males (Figure 5C and D). CPT expression in tissues of *Ascaris suum* (intestinal nematode large enough to perform facile tissue dissection) also shows much higher expression in ovary compared to both uterus in female worms and the seminal vesicle and testis in males (Figure S45; *A. suum* RNAseq normalized expression values are from Rosa et al, 2014).[31] The *in vivo* screening results and the RNAseq expression profiles support the overall observation that the **P1** target plays a critical role in egg production.

CONCLUSIONS

Nematode parasites have evolved over millions of years to occupy a wide variety of ecological and trophic niches. Nematoda is an ancient phylum with the estimated time since last common ancestors with other animal phyla being traced to the Cambrian explosion ~550 million years ago.[32–33] As the consequence of this complex natural history, discovery of drugs that exhibit activity against a broad spectrum of species of parasitic nematodes that are only very distantly related to each other is challenging. Nonetheless, there is a pressing need for novel, broadly effective anthelmintics, especially given that multiple concurrent infections occur in many regions.[34] Here, starting with a single compound perhexiline (**PHX**) that has been reported to display pan-phylum potential as anti-parasitic by Taylor et al. 2013,[12] we identified diverse classes of chemical compounds that are effective against an array of divergent nematodes encompassing different modes of parasitism – intestinal and tissue-dwelling. These inhibitors display *in vitro* whole worm assay IC_{50} values similar to anthelmintics that are currently most commonly used.[35] Notably, even though anthelmintic activity have not been previously attributed to these compounds, many of the prioritized compounds that we rationally selected for screening displayed significant anthelmintic activity against one or more species of nematodes.

Herein, \we have shown that several series of previously known CPT modulators and newly designed compounds significantly affect the motility and viability of several types of parasitic worms in phenotypic assays of worm motility. It remains unclear whether the relative differences among species is a result of variable inhibition of the nematode CPT enzymes or is due to differential outer membrane penetration of the worms. Since, we only performed phenotypic screening on whole worms, it is plausible that one or more of these new chemical series of nematode inhibitors do not target CPTs and the effect is derived from other biological targets or activities. However, our findings from drug bioaccumulation screening suggest that some inactive analogs are incapable of penetrating the cuticle of the nematode. This knowledge can be directed at improving uptake of inhibitors through the neamtode cuticle and used to optimize the compounds for potency.

To conclude, we report the discovery of multiple series of small molecules as novel anthelmintics with pan-phylum anti-nematode activity. Following a rationally guided repurposing strategy of small molecule human CPT inhibitors, we have successfully identified several new chemical classes of pan-nematode inhibitors. Since our data were generated via phenotypic screening, additional investigation is needed to identify their mechanism of action. It is possible that the different chemical series might have diverse targets, some of which may include nematode CPT enzymes. Nevertheless, our results from this study now enable and facilitate the optimization of these lead novel small molecule inhibitors as innovative drugs to treat a variety of debilitating diseases caused by parasitic worms.

METHODS

Ethics statement

All animal experiments were carried out under protocols approved by University of Massachusetts Medical School (UMMS; A-2483 and A-2484) Institutional Animal Care and Use Committees (IACUC). All housing and care of laboratory animals conformed to the National Institutes of Health (NIH) Guide for the Care and Use of Laboratory Animals in Research (see 18-F22) and all requirements and all regulations issued by the United States Department of Agriculture (USDA), including regulations implementing the Animal Welfare Act (P.L. 89-544) as amended (see 18-F23). Euthanasia was accomplished by CO_2 asphyxiation, followed by bilateral pneumothorax.

Identifying known small molecule CPT modulators

CPT orthologs were identified using orthoMCL[36] over predicted proteomes of 23 species. The proteomes selected belonged to 14 nematodes – including STHs, filariids and strongylids – and nine outgroup species (Table S1). An inflation factor of 1.5 was used. CPT genes of *C. elegans* were used to identify CPT orthologs in the other species. Normalized *A. ceylanicum* CPT expression levels for Fig. 5C and 5D were extracted from developmental global expression profile table available at Nematode.net[37] and normalized *A. suum* CPT expression levels for Figure S1 were extracted from Rosa et al, 2014.[31]

CPT orthologs among the target proteins in ChEMBL database v18 were identified using BLAST (e-10, 50% identity) identifying 105 ChEMBL compounds targeting these proteins (Table S2). Compound clustering was accomplished based on structural similarity using FP2 fingerprints in Open Babel (v2.3).[38] The physicochemical score was assigned based on an approach reported previously,[12] with a minimum score of 4 being required for selection. Information on commercial availability of test compounds was sourced from the ZINC database.[39]

Homology models were built for four worm and three mammalian host species using Molecular Operating Environment software (Chemical Computing Group, Montreal, version 2014.09). CPT sequences from the nematodes *T. muris, A. ceylanicum, C. elegans, S. stercoralis* and the mammals *M. musculus, M. auratus*, and *H. sapiens*, were aligned with the crystal structures from *R. norvegicus* CPT2 (2FW3).[40] This structure includes the ligand teglicar[41] in the binding site. The homology models were built individually, with the teglicar atoms included to maintain reasonable binding site geometry. Each model was energy minimized using the AMBER10 force field.[42] Resulting models were compared to several other rat CPT2 crystal structures (2DEB, 2FYO, 2H4T, 4EP9, 4EPH, 4EYW) with no significant differences in the region of the binding site. Ligand docking to any of the models was done using FRED (OpenEye Scientific Software, Santa Fe, version 3.0.1), followed by energy minimization in the AMBER10 force field.

Compound screening with intestinal nematodes

A. ceylanicum: *In vitro* assays were carried out as previously described.[35] Three adult worms were manually sorted into each wells of 96-well plate, containing culture medium

and the test drug (4 wells/test drug). Primary CPT inhibitors were tested against hookworm at 1, 3, 10, 40 and 80 μg/ml in 1% DMSO. Analogs of **6a** and **10a** were tested at 250 μM and 125 μM. Worms were scored for motility after 24 hours of incubation at 37°C and 5% CO_2.

T. muris: *In vitro* assays were carried out as described.[35] Four worms were manually sorted into each well of 24-well plates (3 wells/ test drugs). Primary CPT inhibitors were tested against whipworms at 40 and 80 μg/ml and the analogs of **6a** and **10a** were tested at 250 μM and 125 μM. Worms were scored for motility after 48 hours of incubation at 37°C and 5% CO_2. IC50 determinations were conducted at 500 μM, 250 μM, 125 μM, 62.5 μM, 31.25 μM, 15.6 μM, 7.8 μM, 3.9 μM, 1.9 μM, 0 μM. IC50 values at 48 hours were used to establish a non-linear regression using Prism 7 (Graphpad, La Jolla, CA). All *T. muris* IC50s listed displayed R^2 values ≥0.8.

H. polygyrus: 4 weeks old Swiss Webster mice (females) were infected by stomach gavage with infective L3 of *H. polygyrus*, 15 days post infection parasites were harvested from the small intestine and four worms were manually sorted into each well of 96-well plates (three wells/test drugs) containing nematode culture medium and test drugs at 80 and 40 μg/ml in 1% DMSO. Worms were scored for motility after 72 hours of incubation at 37°C and 5% CO_2.

N. brasiliensis: 5 weeks old laboratory rats were infected with iL3 of *N. brasiliensis* by the subcutaneous route. Six days post infection, the rats were euthanized and parasites were harvested from the small intestine and four worms were manually sorted into each well of 96-well plates (four wells/ test drugs) containing nematode culture medium and test drugs at 80 and 40 μg/ml in 1% DMSO. Worms were scored for motility after 48 hours of incubation at 37°C and 5% CO_2.

Ex vivo drug activity was determined using the standard motility index ranging from 0–3 as previously described.[35] Motility index of 3 were given to vigorous worms, 2 for motile worms, 1 for motile after stimulation by touching, and 0 for dead worms.

Compound screening with the filarial nematode *B. pahangi*

Adult female *B. pahangi* worms were obtained from Dr. Brenda Beerntsen, University of Missouri, Columbia, MO. Individual females were placed in each well of a 24-well plate in culture medium (RPMI-1640 with 25 mM HEPES, 2.0 g/L NaHCO3, 5% heat inactivated FBS, and 1× Antibiotic/Antimycotic solution). Excess medium was removed, leaving 500 μL in each well.

Fresh powders of the seven known CPT inhibitors that were synthesized (**6a**, **10a–c** and **17a–b**) were dissolved in DMSO (Fisher Scientific, Fair Lawn, NJ). Initial screening of the compounds was performed at 100 μM and at 20 μM. Four worms were used as replicates at each concentration. Worms treated with 1% DMSO only served as the negative control. The cultures were maintained at 37°C, 5% CO_2 incubator for seven days; the duration of the assay.

The Worminator, a visual imaging software system developed and described previously was used to determine the effect of each treatment on worm motility.[43] Movements of individual worms were calculated by determining the number of pixels displaced per second per well. Worm movements were averaged over the time of recording (60 seconds) and mean movement units (MMUs) were determined for individual worms. Percent inhibition of motility was calculated by dividing the MMUs of the treated worms by the average MMUs of the 1% DMSO treated control worms, subtracting the value from 1.0, flooring the values to zero and multiplying by 100%. Videos of the worms during the assay were recorded on days 0, 1, 2, 3, and 6 of the incubation. Compounds showing ≥75% inhibition of motility at either concentration on day 3 of the assay were investigated further using IC_{50} assay. Compounds **6a** and **10a** at 100μM fit this criterion, inhibiting worm motility 95% and 100%, respectively, on day 3. IC_{50} determinations were conducted at 100 μM, 30 μM, 10 μM, 3 μM, 1 μM, 0.3 μM. Worms were treated in the same fashion as above and motility was measured each day for three days using the Worminator. IC50 values on day 2 was used to establish a non-linear regression curve fit, using Prism 7 (Graphpad, La Jolla, CA). All *Brugia* IC_{50}s listed in Table S4 all displayed R^2 values ≥0.8.

Bioaccumulation assays

T. muris: Twelve adult *T. muris* worms were placed into three worms/well. The wells contained the drug at a final concentration of 100 μM in 1% DMSO. After 6 hours of incubation, the worms were placed into clean plates containing saline and washed twice. This was followed by three more washes using 0.1% SDS to remove drugs from the surface. The worms were then placed into an Eppendorf tube and washed twice using saline and centrifuged to form a pellet, which was stored overnight at −20°C. At the time of assay, the worms were frozen in liquid Nitrogen, crushed using pestles and incubated with 100 μL of 1× lysis buffer with proteinase K for 60 min at 60°C. Two μL of the worm digestant was used to measure the total protein content using BCA protein kit. The proteins from the remaining digestant were precipitated using 100 μL of acetonitrile. The supernatant (~180 μL) was stored at −80°C. The lysates were analyzed for levels of each individual compound by HPLC/MS analysis. DMSO was used as the negative control while **P1**, which is known to be membrane permeable, was used as the positive control.

Lysates were analyzed on a Hewlett Packard Series 1100 HPLC, using a Sunfire C_{18} 3.5 μm pore-size, 4.6 × 50 mm column. Samples were injected with 10 μL of volume with a flow rate of 1 mL/min, and solvent system of H_2O (0.01% TFA) and acetonitrile (0.05% TFA). Gradient was 0→5 minutes: 5-95% linear increase acetonitrile, 5→6 minutes 95% acetonitrile hold, 6→7 minutes 95-5% linear decrease acetonitrile. Elution was monitored by 210 and 254 nm UV-absorption and by MS. MS conditions were drying gas 12 L/min, drying gas temperature 350° C, nebulizer psig 55–60, and capillary voltage 4000 V. Compound presence was evaluated by extracting $[M+H]^+$ or $[M+Na]^+$ of parent compound mass.

B. *pahangi*: Adult female *B. pahangi* worms were prepared for *in vitro* culture as described above and treated *in vitro* for 72 hours. Upon collection worms were washed twice in 0.1% SDS, followed by 1 wash in culture media, then frozen in culture media at −20° C. To

prepare lysates for bioaccumulation assays, worms were thawed on ice, media was removed, and three to four worms were pooled together. Worms were then washed once with PBS, frozen in liquid nitrogen and crushed with pestles. Lysates were prepared as described for *T. muris* above, with the exception that worms were incubated at 60° C for 5 hours.

Perhexiline *A. ceylanicum in vivo* assay

Experiments were conducted essentially as previously described.[35, 44] Five weeks old golden Syrian hamsters were infected with 100 iL3 of *A. ceylanicum*. Infected rodents were grouped based on the fecal egg count on day 18 post infection. One group was treated with single oral dose of 100 mg/kg Perhexiline (**1**) whereas the other group (control) was dosed only with water. Fecal samples were collected 20 days post infection (p.i) for fecal egg count. On day 21 p.i., the hamsters were euthanized and the small intestine opened longitudinally. Adult parasites within the intestine were counted under a dissecting microscope.

COMPOUND SYNTHESIS

General Methods

Starting materials, reagents, and solvents were purchased from commercial vendors unless otherwise noted. In general, anhydrous solvents were used for carrying out all reactions. ^{1}H and ^{13}C NMR spectra were measured on a Varian 400 MHz NMR instrument equipped with an auto sampler. The chemical shifts were reported as δ ppm relative to TMS using residual solvent peak as the reference unless otherwise noted. The following abbreviations denote the peak multiplicities: s = singlet; d = doublet; t = triplet; q = quartet; m = multiplet; br = broad. All reactions were monitored by thin layer chromatography (TLC) carried out on either Merck silica gel plates (0.25 mm thick, 60F254) and visualized by using UV (254 nm) or dyes such as phosphomolybdic acid. Silica gel chromatography was carried out on a Teledyne ISCO CombiFlash purification system using pre-packed silica gel columns (4 g–24 g sizes).

General procedures

General procedure for compounds 6a and 6f: Method A—Compound **4a**[45] (0.180 g, 0.52 mmol) was dissolved in trifluoroacetic acid (1 mL), stirred 1 h, then concentrated *in vacuo* to provide intermediate **5a**, which was dissolved in anhydrous DCM (2 mL) and the solution was bubbled with argon 2 min, then triethylamine (0.29 mL, 2.1 mmol) and DMAP (0.006 g, 0.05 mmol) were added, followed by phenoxyacetyl chloride (0.072 mL, 0.52 mmol). The mixture was stirred 24h at RT, then washed with water, then brine, dried with Na_2SO_4, and concentrated in vacuo, after which it was purified by silica gel chromatography with ethyl acetate/hexanes combinations as eluent, giving rise to the title compound **6a**.

General procedure for compounds 6(b–e) & 6(g–k): Method B—CDI (66 mg, 0.4 mmol) was added into a solution of 2-phenoxyacetic acid (31 mg, 0.2 mmol) in DCM (2 mL) and solution was stirred for 30 min at room temperature; thereafter, solution of (R)-2-(piperidin-2-yl)-4-(pyridin-2-yl, **5a**[45] (50 mg, 0.2 mmol) in DCM (1 mL) was added and the reaction solution stirred for 24h. Progress of the reaction was monitored by TLC and upon

completion of the reaction, reaction mass diluted with DCM (10 mL), washed with 10% citric acid, followed by saturated $NaHCO_3$ and brine. The organic layer was dried over anhydrous Na_2SO_4. Solvent was evaporated under reduced pressure and the crude compound was subjected for column chromatography.

General procedure for compounds 6(l–m): Method C—To a solution of 2-phenoxy acetic acid (120 mg, 0.57 mmol), there was added HOBt (231 mg, 1.71 mmol) and EDC (265 mg, 1.71 mmol, 3 eq) at 0°C in 20 mL of THF, and allowed to stir for 15 minutes. To this solution there was then added the amine **5a** (135 mg, 0.57 mmol) and triethylamine (99 μL, 0.7 mmol). The solution was allowed to stir overnight and reach room temperature. The reaction was then diluted with EtOAc, and washed with 1M HCl, brine, and dried over Na_2SO_4. The ester was purified by silica gel column chromatography using EtOAc/hexanes to provide the compounds **6(l–m)**. The methyl ester **6(l–m)** was dissolved in methanol/water (1:1 v/v) and three equivalents of LiOH were added and the solution stirred until the methyl ester was fully hydrolyzed. The majority of the methanol was removed *in vacuo* and the resulting solution was extracted with EtOAc, dried with Na_2SO_4, and concentrated under reduced pressure. The crude compounds were purified by silica gel column chromatography using EtOAc/hexanes to provide the compounds **6(m–o)**.

(R)-2-phenoxy-1-(2-(4-(pyridin-2-yl)thiazol-2-yl)piperidin-1-yl)ethan-1-one (6a):

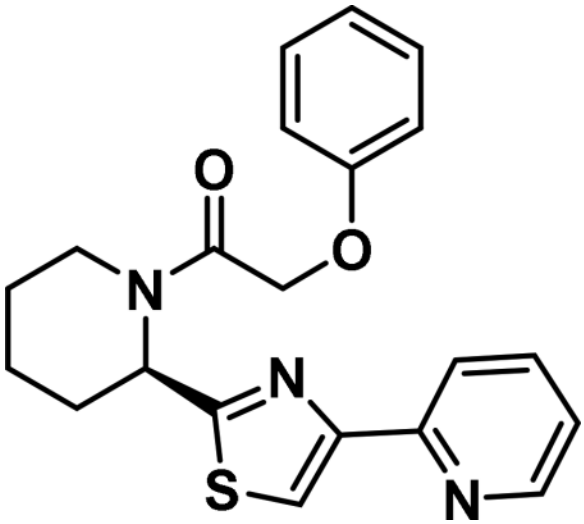

Compound synthesized as per method A, white solid with 170 mg in 86% yield; ^{1}H NMR (400 MHz, CD_3Cl) δ ppm 8.94 (d, *J* = 5.5 Hz, 1 H), 8.57 (s, 1 H), 8.31-8.23 (m, 1 H), 8.14 (t, *J* = 7.4 Hz, 1 H), 7.56 (t, *J* = 6.3Hz, 1 H), 6.05 (d, *J* = 4.7 Hz, 1 H), 4.76 (s, 2 H), 3.91 (d, *J* = 13.3 Hz, 1 H), 3.21 (t, *J* = 12.7 Hz, 1 H), 2.51 (d, *J* = 13.7 Hz, 1 H), 1.93-1.79 (m, 1 H), 1.77-1.58 (m, 3 H), 1.58-1.35 (m, 1 H) (rotamers); LCMS (ESI): found $[M + H]^+$, 380.3.

(R)-2-([1,1'-biphenyl]-4-yloxy)-1-(2-(4-(pyridin-2-yl)thiazol-2-yl)piperidin-1-yl)ethan-1-one (6b):

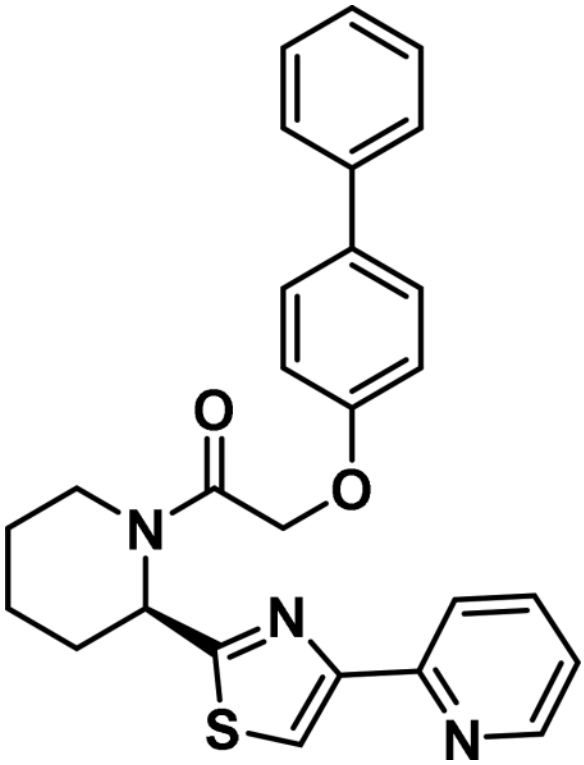

Compound synthesized as per method B, white solid with 37 mg in 40% yield; ^{1}H NMR (400 MHz, CD_3Cl) δ ppm 9.15 (br. s., 1 H), 8.63-8.52 (m, 1 H), 8.23 (d, *J* = 7.8 Hz, 1 H), 7.52 (br. s., 4 H), 7.47 (br. s., 1 H), 7.45-7.36 (m, 3 H), 7.36-7.28 (m, 1 H), 7.08 (d, *J* = 8.2 Hz, 2 H), 6.99 (d, *J* = 8.6 Hz, 1 H), 6.14 (d, *J* = 4.3 Hz, 1 H), 4.88 (d, *J* = 3.1 Hz, 2 H), 3.98 (d, *J* = 16.8 Hz, 1 H), 3.46 -3.30 (m, 1 H), 2.72-2.52 (m, 1 H), 2.29-2.01 (m, 3 H), 1.94 (dd, *J* = 18.2, 6.1 Hz, 2 H), 1.80 (br. s., 3 H), 1.72 (br. s., 1 H),1.68-1.49 (m, 2 H), 1.35-1.17 (m, 2 H), 0.93-0.77 (m, 1 H)(rotamers); LCMS (ESI): found $[M + H]^{+}$, 456.3.

(R)-2-(naphthalen-1-yloxy)-1-(2-(4-(pyridin-2-yl)thiazol-2-yl)piperidin-1-yl)ethan-1-one (6c):

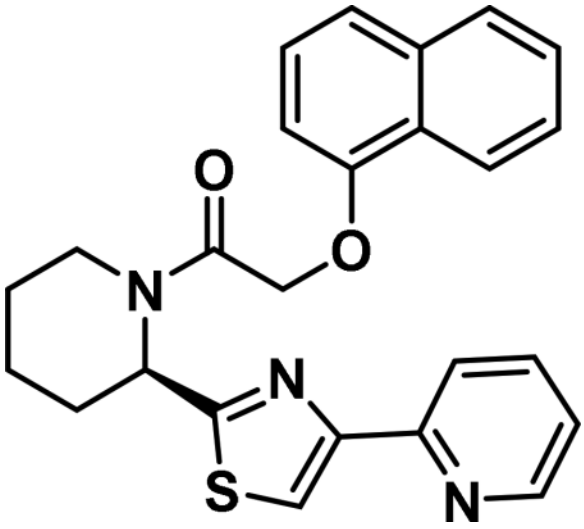

Compound synthesized as per method B, white solid with 32 mg in 41% yield; ^{1}H NMR (400 MHz, CD_3Cl) δ ppm 9.14 (br. s., 1 H), 8.57 (br. s., 1 H), 8.32 (d, *J* = 7.4 Hz, 1 H), 8.24-8.10 (m, 1 H), 7.83 (d, *J* = 6.7 Hz, 1 H), 7.60-7.45 (m, 4 H), 7.45-7.31 (m, 4 H), 6.95 (d, *J* = 6.3 Hz, 1 H), 6.17 (br. s., 1 H), 5.11-4.94 (m, 2 H), 4.21-4.00 (m, 1 H), 3.49-3.27 (m, 1 H), 2.70-2.56 (m, 1 H), 1.83-1.67 (m, 3 H), 1.67-1.46 (m, 1 H), 1.27 (br. s., 1 H) (rotamers); LCMS (ESI): found $[M + H]^+$, 430.3.

2-(naphthalen-2-yloxy)-1-((2R)-2-(4-(pyridin-2-yl)-4,5-dihydrothiazol-2-yl)piperidin-1-yl)ethan-1-one (6d):

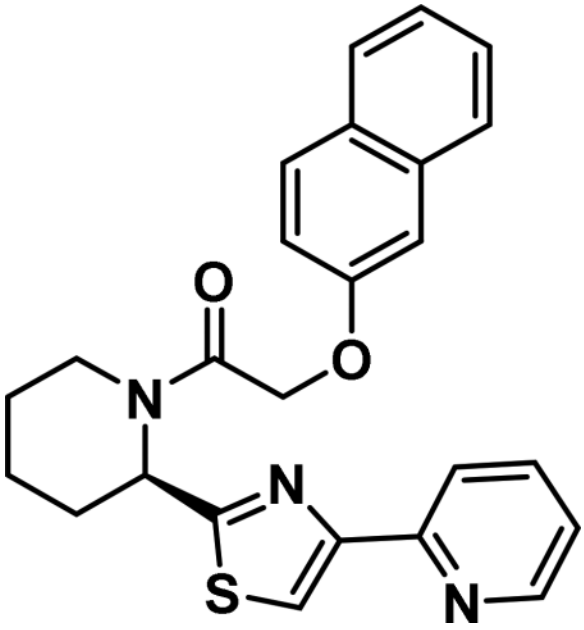

Compound synthesized as per method B, white solid with 18 mg in 41% yield; ^{1}H NMR (400 MHz, CD_3Cl) δ ppm 9.28 (br. s., 1 H), 8.71 (d, *J* = 4.3 Hz, 1 H), 8.57 (d, *J* = 8.2 Hz, 1 H), 7.84-7.74 (m, 2 H), 7.74-7.52 (m, 4 H), 7.48-7.29 (m, 3 H), 7.26-7.10 (m, 3 H), 6.15 (d, *J* = 5.1 Hz, 1 H), 4.96 (s, 2 H), 4.08 (d, *J* = 13.3 Hz, 1 H), 3.35 (t, *J* = 12.7 Hz, 1 H),

2.65-2.51 (m, 1 H), 2.03 -1.87 (m, 1 H), 1.86-1.68 (m, 3 H), 1.68-1.49 (m, 1 H)(rotamers); LCMS (ESI): found $[M + Na]^+$, 430.3.

2-(4-((3R,5R,7R)-adamantan-1-yl)phenoxy)-1-((R)-2-(4-(pyridin-2-yl)thiazol-2-yl)piperidin-1-yl)ethan-1-one (6e):

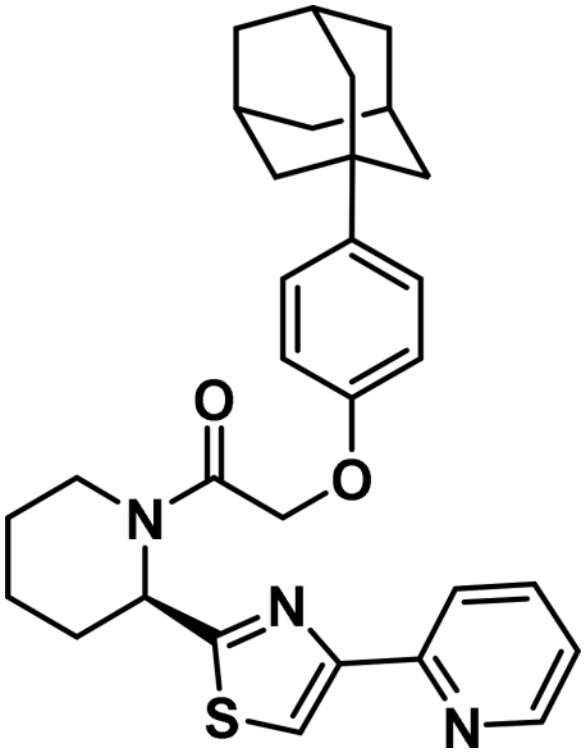

Compound synthesized as per method B, white solid with 24 mg in 46% yield; ^{1}H NMR (400 MHz, CD_3Cl) δ ppm 9.14 (br. s., 1 H), 8.58 (br. s., 1 H), 8.20 (d, *J* = 7.0 Hz, 1 H), 7.52 (s, 1 H), 7.42-7.32 (m, 1 H), 7.23 (d, *J* = 7.8 Hz, 1 H), 6.95 (d, *J* = 8.2 Hz, 1 H), 6.87 (d, *J* = 7.4 Hz, 1 H), 6.12 (br. s., 1 H), 4.80 (d, *J* = 7.4 Hz, 2 H), 3.95 (d, *J* = 12.9 Hz, 1 H), 3.43-3.28 (m, 1 H), 2.62 (d, *J* = 11.7 Hz, 1 H), 2.09 (br. s., 4 H), 1.97-1.80 (m, 10H), 1.26 (br. s., 5 H), 0.88 (d, *J*=10.2 Hz, 1 H)(rotamers); LCMS (ESI): found $[M + Na]^+$, 514.4.

(R)-2-(4-methoxyphenoxy)-1-(2-(4-(pyridin-2-yl)thiazol-2-yl)piperidin-1-yl)ethan-1-one (6f):

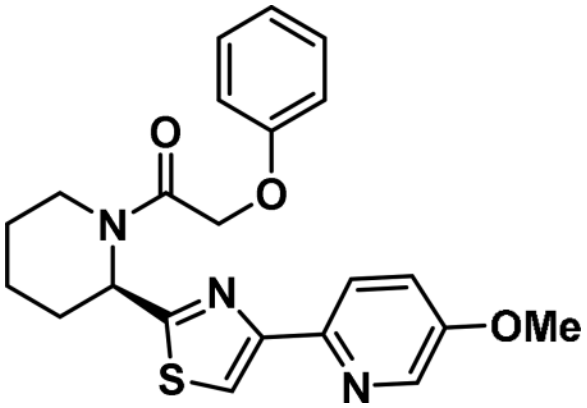

Compound synthesized as per method A, white solid with, 176 mg in 86% yield; ^{1}H NMR (400 MHz, CD_3Cl) δ ppm 7.83 (d, *J* = 8.2 Hz, 2 H), 7.37-7.27 (m, 2 H), 7.26-7.20 (m, 1 H), 7.05-6.91 (m, 5 H), 6.12 (br. s., 1 H), 4.94-4.76 (m, 2 H), 3.91 (d, *J* = 13.3 Hz, 1 H), 3.86 (s, 3 H), 3.38 (t, *J* = 13.1 Hz, 1 H), 2.62 (d, *J* = 12.1 Hz, 1 H), 2.08-1.91 (m, 1 H), 1.84 (d, *J* = 14.1 Hz, 1 H), 1.73 (d, *J* = 12.5 Hz, 2 H), 1.65-1.56 (m, 1 H), 1.56-1.39 (m, 1 H)(rotamers); LCMS (ESI): found $[M + H]^{+}$, 410.4.

(R)-2-(4-cyclohexylphenoxy)-1-(2-(4-(pyridin-2-yl)thiazol-2-yl)piperidin-1-yl)ethan-1-one (6g):

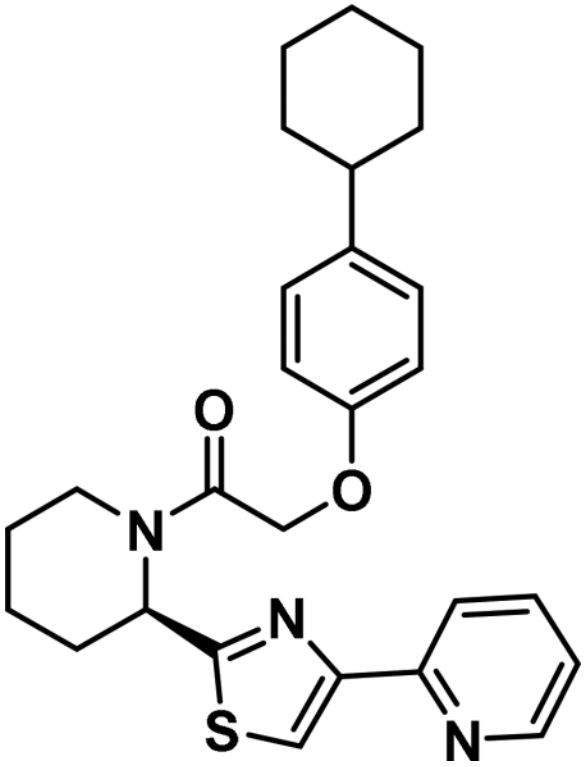

Compound synthesized as per method B, white solid with 21 mg in 45% yield; ^{1}H NMR (400 MHz, CD_3Cl) δ ppm 9.13 (br. s., 1 H), 8.58 (br. s., 1 H), 8.28-8.03 (m, 1 H), 7.52 (br. s., 1 H), 7.36 (br. s., 1 H), 7.22 -7.02 (m, 2 H), 7.02-6.88 (m, 1 H), 6.85 (br. s., 1 H), 6.12 (br.

s., 1 H), 4.76 (br. s., 2 H), 3.96 (d, *J* = 9.0 Hz, 1 H), 2.63 (d, *J* = 10.6 Hz, 1 H), 2.54-2.25 (m, 1 H), 1.83 (br. s., 5 H), 1.76 (br. s., 4 H), 1.37 (br. s., 6 H), 1.26 (br. s., 6 H), 0.87 (d, *J* = 10.6 Hz, 1 H)(rotamers); LCMS (ESI): found $[M + H]^+$, 462.4.

(R)-2-(4-benzylphenoxy)-1-(2-(4-(pyridin-2-yl)thiazol-2-yl)piperidin-1-yl)ethan-1-one (6h):

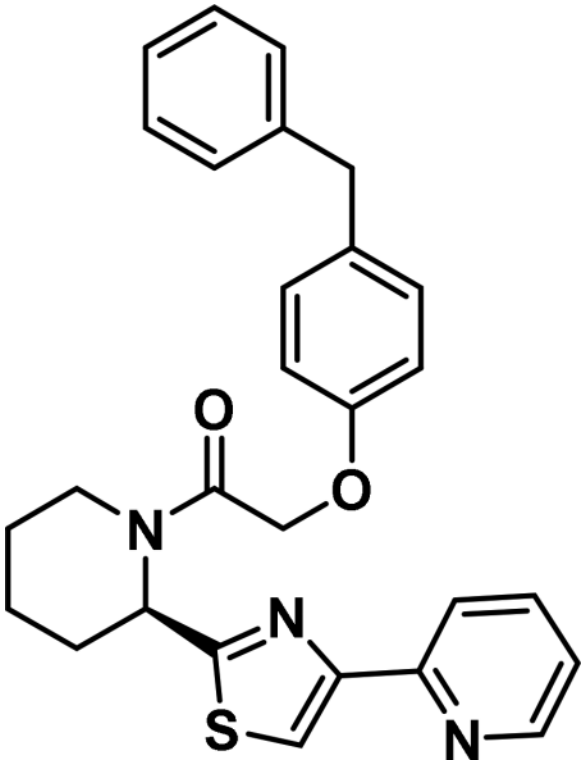

Compound synthesized as per method B, white solid with 24 mg in 50% yield; ^{1}H NMR (400 MHz, CD_3Cl) δ ppm9.34 (br. s., 1 H), 8.79-8.64 (m, 2 H), 7.85-7.74 (m, 1 H), 7.67 (s, 1 H), 7.35-7.29 (m, 1 H), 7.25-7.02 (m, 5 H), 6.93 (d, *J* = 8.2 Hz, 1 H), 6.11 (d, *J* = 4.3 Hz, 1 H), 4.81 (br. s., 2 H), 3.99 (d, *J* = 14.1 Hz, 1 H), 3.95-3.85 (m, 2 H), 3.27 (t, *J* = 12.9Hz, 1 H), 2.55 - 2.68 (m, 1 H), 2.11-1.87 (m, 1 H), 1.83-1.53 (m, 4 H)(rotamers); LCMS (ESI): found $[M + H]^+$, 470.4.

(R)-2-((4'-methyl-[1,1'-biphenyl]-4-yl)oxy)-1-(2-(4-(pyridin-2-yl)thiazol-2-yl)piperidin-1-yl)ethan-1-one (6i):

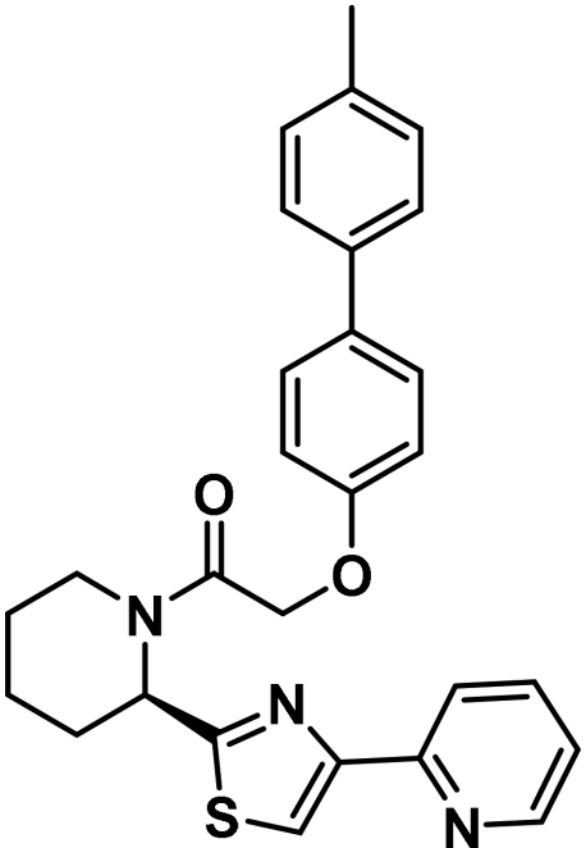

Compound synthesized as per method B, white solid with 12 mg in 42% yield; ^{1}H NMR (400 MHz, CD_3Cl) δ ppm 9.13 (br. s., 1 H), 8.56 (br. s., 1 H), 8.23-8.13 (m, 1 H), 7.59 (br. s., 1 H), 7.51 (d, *J* = 7.0 Hz, 3 H), 7.47-7.39 (m, 3 H), 7.39-7.30 (m, 2 H), 7.26-7.15 (m, 3 H), 7.06 (d, *J* = 7.4 Hz, 1 H), 7.03-6.88 (m, 1 H), 6.14 (br. s., 1 H), 4.87 (br. s., 2 H), 3.98 (d, *J* = 5.5 Hz, 1 H), 3.44-3.32 (m, 1 H), 2.77-2.53 (m, 1 H), 2.39 (br. s., 4 H), 1.91-1.67 (m, 3 H), 0.96-0.77 (m, 4H)(rotamers); LCMS (ESI): found $[M + H]^+$, 470.4.

(R)-2-(4-(pyridin-2-yl)phenoxy)-1-(2-(4-(pyridin-2-yl)thiazol-2-yl)piperidin-1-yl)ethan-1-one (6j):

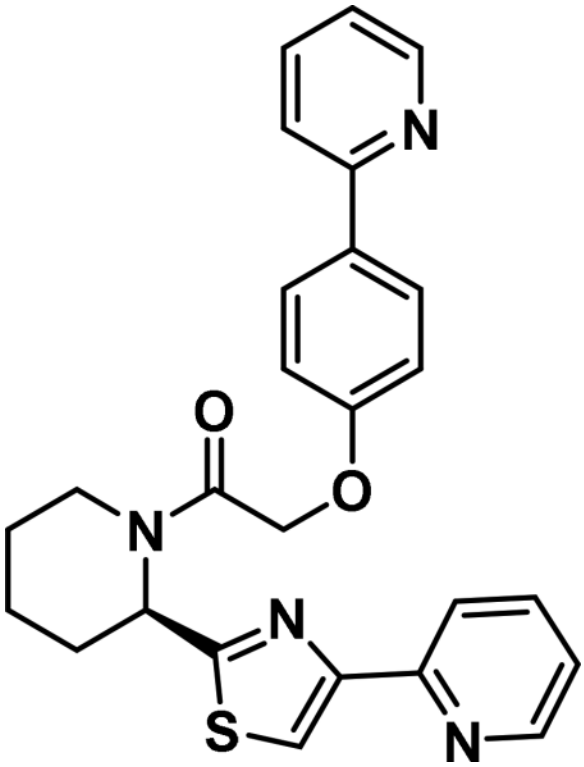

Compound synthesized as per method B, white solid with 50 mg in 41% yield; ^{1}H NMR (400 MHz, CD_3Cl) δ ppm9.13 (br. s., 1 H), 8.66 (br. s., 1 H), 8.56 (br. s., 1 H), 8.17 (d, *J* = 6.7 Hz, 1 H), 7.85-8.01 (m, 2 H), 7.80-7.62 (m, 2 H), 7.52 (br. s., 1 H), 7.35 (br. s., 1 H), 7.21 (br. s., 1 H), 7.10 (d, *J* = 7.8 Hz, 1 H), 7.02 (d, *J* = 7.0 Hz, 1 H), 6.13 (br. s., 1 H), 4.08-3.90 (m, 1 H), 3.38 (t, *J* = 12.7 Hz, 1 H), 2.73-2.56 (m, 1 H), 2.03 (d, *J* = 18.4 Hz, 2 H), 1.97-1.86 (m, 1 H), 1.78 (br. s., 2 H), 1.70 (br. s., 1 H), 1.65-1.45 (m, 1 H), 1.26 (br. s., 2 H) (rotamers); LCMS (ESI): found $[M + H]^+$, 457.3.

(R)-1-(2-(4-(naphthalen-2-yl)thiazol-2-yl)piperidin-1-yl)-2-phenoxyethan-1-one (6k):

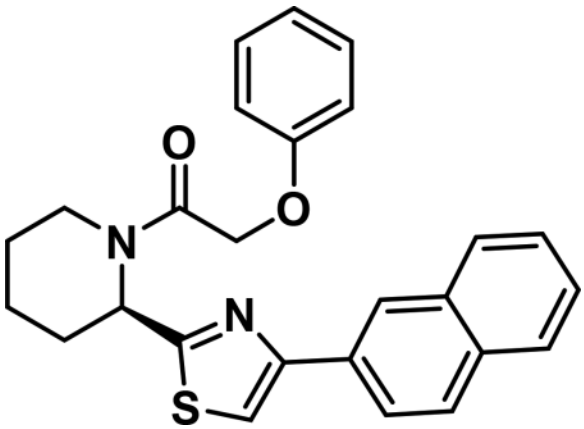

Compound synthesized as per method B, white solid with 20 mg in 50% yield; ^{1}H NMR (400 MHz, CD_3Cl) δ ppm 8.45 (s, 1 H), 8.03 (d, *J* = 8.6 Hz, 1 H), 7.93-7.82 (m, 4 H), 7.53-7.43 (m, 2 H), 7.30-7.20 (m, 1 H), 7.14 (t, *J* = 7.6 Hz, 1 H), 7.02 (d, *J* = 7.8 Hz, 1 H),

6.95 (d, *J* = 7.8 Hz, 2 H), 6.08 (d, *J* = 4.3 Hz, 1 H), 5.07-4.91 (m, 2 H), 3.95 (d, *J* = 13.7 Hz, 1 H), 3.41 (t, *J* = 13.1 Hz, 1 H), 2.72 - 2.47 (m, 1 H), 2.03-1.90 (m, 1 H), 1.83-1.61 (m, 4 H) (rotamers); LCMS (ESI): found $[M + H]^+$, 429.3

(R)-2-((4-methylbenzoate)phenoxy)-1-(2-(4-(pyridin-2-yl)thiazol-2-yl)piperidin-1-yl)ethan-1-one (6l):

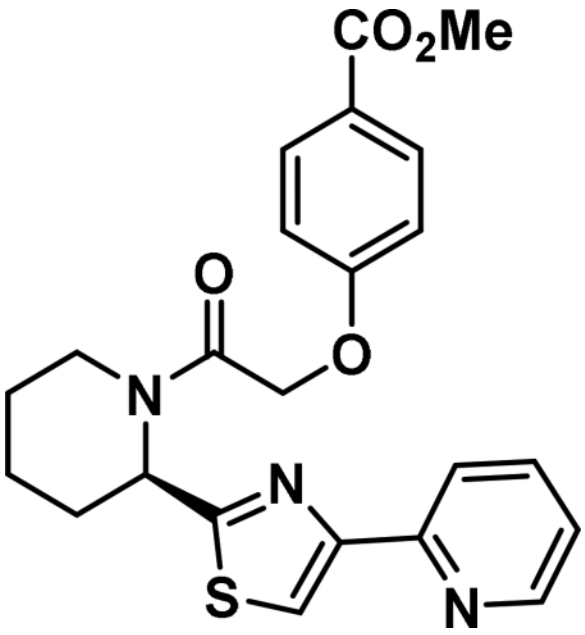

Compound synthesized as per method C, white solid with 140 mg in 65% yield. ^{1}H NMR (400 MHz, CD_3OD)δ ppm: 9.39-9.12 (m, 1H), 9.04-8.81 (m, 1H); 8.77-8.66 (m, 1H), 8.39-8.21 (m, 1H), 8.06-7.71 (m, 3H), 7.10-6.84 (m, 2H), 6.10-5.20 (m, 1H), 5.10 (m, 2 H), 4.50-3.90 (m, 1H), 3.87-3.77 (m, 3 H), 3.30 (m, 1 H), 2.98-1.46 (m, 7 H)(rotamers); LCMS (ESI): found $[M+H]^+$, 438.3

(R)-2-(3-methylbenzoatephenoxy)-1-(2-(4-(pyridin-2-yl)thiazol-2-yl)piperidin-1-yl)ethan-1-one (6m):

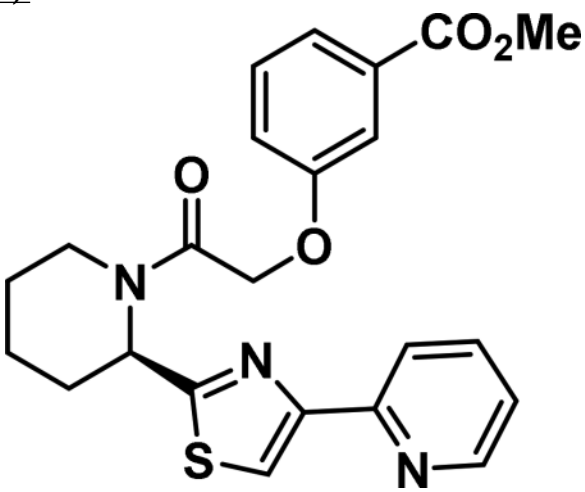

Compound synthesized as per method C, white solid with 135 mg, 63% yield. ^{1}H NMR (400 MHz, CD_3OD)δ ppm 9.17-9.02 (m, 1H), 8.53-8.43 (m, 1H), 8.35 (m, 1 H), 8.11-7.96 (m, 1 H), 7.67-7.58 (m, 1 H), 7.56-7.44 (m, 2H), 7.42-7.11 (m, 2 H), 6.15-5.6 (m, 1 H), 5.00 (m, 2H), 4.0-4.50 (m, 1H), 3.91-3.79 (m, 3H), 3.40-2.50-3.4 (m, 2H), 2.04-1.17 (m, 7 H) (rotamers); LCMS (ESI): found $[M+H]^+$, 438.3

(R)-2-((4-benzoic acid)phenoxy)-1-(2-(4-(pyridin-2-yl)thiazol-2-yl)piperidin-1-yl)ethan-1-one (6n):

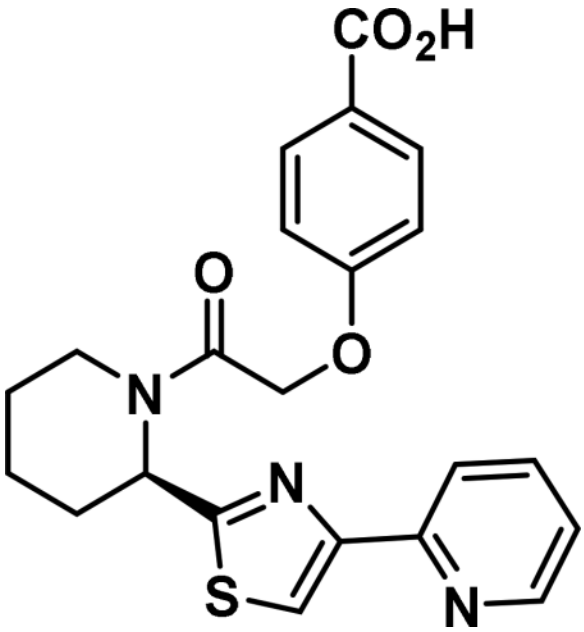

Compound synthesized as per method C, white solid with 43 mg, 88% yield. ^{1}H NMR (400 MHz, CD_3OD) δ ppm 9.30-9.01 (m, 1 H), 8.85-8.49 (m, 2 H), 8.28-8.05 (m, 1 H), 7.90-7.61 (m, 3 H), 7.10-6.73 (m, 2 H), 6.13-5.51 (m, 1 H), 5.00 (m, 2 H), 4.54-3.77 (m, 1 H), 3.45-2.72 (m, 1 H), 2.64-1.32 (m, 7 H) (rotamers); LCMS (ESI): found $[M+H]^+$, 424.3

(R)-2-((3-benzoic acid)phenoxy)-1-(2-(4-(pyridin-2-yl)thiazol-2-yl)piperidin-1-yl)ethan-1-one (6o):

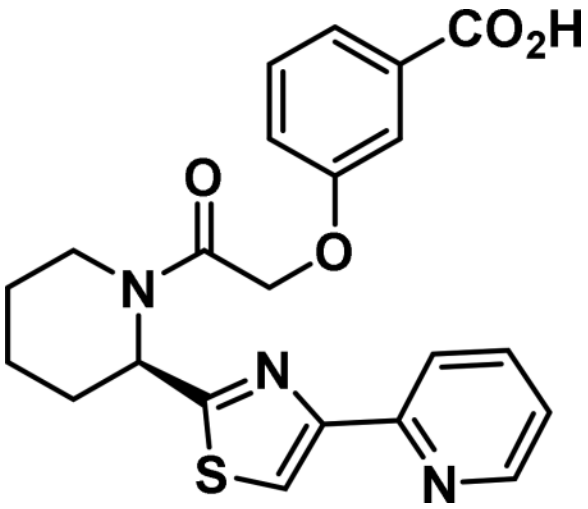

Compound synthesized as per method C, white solid with 35 mg, 72% yield. ^{1}H NMR (400 MHz, CD_3OD) δ ppm 9.23-8.99 (m, 1 H), 8.64-8.43 (m, 1 H), 8.43-8.20 (m, 1 H), 8.06-7.99 (m, 1 H), 7.95-7.81 (m, 1 H), 7.87-7.69 (m, 1 H), 7.67-7.59 (m, 1 H), 7.58-7.43 (m, 3 H), 7.43-7.12 (m, 2 H), 6.20-5.51 (m, 1 H), 5.00 (m, 2 H), 4.60-3.90 (m, 1 H), 3.45-2.60 (m, 1 H), 1.86-0.79-(m, 8 H) (rotamers); LCMS (ESI): found $[M+H]^+$, 424.3

General procedure for compounds 9(a–c): Method D—Under nitrogen atmosphere, dry DCM (7.5 mL) was added to a flask containing methyl 3-aminobenzoate (0.200 g, 1.3 mmol), then pyridine (0.41 mL, 5.1 mmol) was added. 3,4-dichlorobenzenesulfonyl chloride (0.16 mL, 1.0 mmol) was added dropwise, then the solution was stirred for 3 h at RT. The mixture was poured into excess water and extracted with DCM. The organic layers were combined, washed with aqueous 1N HCl, dried with Na_2SO_4, and concentrated in vacuo. The resulting residue was purified by silica gel chromatography with hexane/ethyl acetate combinations as eluent, giving rise to methyl 3-((3,4-dichlorophenyl)sulfonamido)benzoate (0.262 g) in 71% yield. MS (ESI): found $[M + H]^+$, 360.1. This material was dissolved in methanol/water (1/1 v/v) and three equivalents of LiOH were added and the solution was stirred until the methyl ester was fully hydrolyzed. The majority of methanol was removed in vacuo and the resulting solution was extracted with EtOAc, dried with Na_2SO_4, and concentrated in vacuo, giving rise to 3-((3,4-dichlorophenyl)sulfonamido)benzoic acid **9a**.

3-((3,4-dichlorophenyl)sulfonamido)benzoic acid (9a):

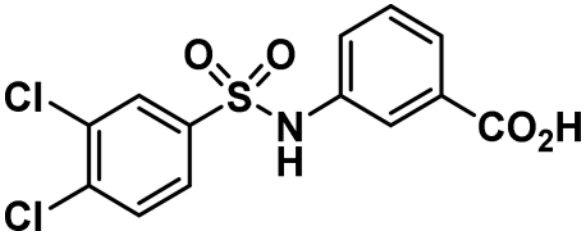

Compound synthesized as per method D, white solid with 189 mg in 75% yield; ^{1}H NMR (400 MHz, $CDCl_3$) δ ppm 7.85-7.79 (m, 1H), 7.75-7.69 (m, 2H), 7.42 (d, J = 8.61 Hz, 2H), 7.40-7.34 (m, 1H), 7.03 (s, 1H); LCMS (ESI): found $[M + H]^+$, 346.2.

3-((4-chlorophenyl)sulfonamido)benzoic acid (9b):

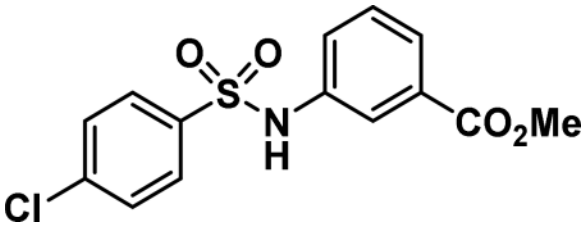

Compound synthesized as per method D, white solid with 155 mg in 80% yield; ^{1}H NMR (400 MHz, $CDCl_3$) δ ppm 7.86-7.78 (m, 1H), 7.75-7.65 (m, 3H), 7.42 (d, *J* = 8.61 Hz, 2H), 7.39-7.35 (m, 1H), 7.02 (s, 1H); LCMS (ESI): found $[M + Na]^+$, 334.2.

3-((5-chloro-2-methoxyphenyl)sulfonamido)benzoic acid (9c):

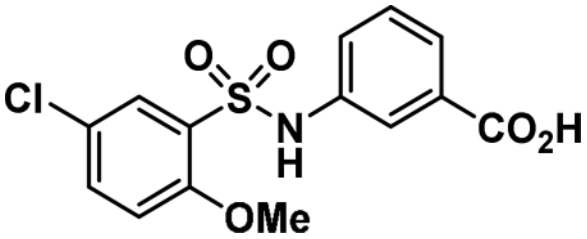

Compound synthesized as per method D, white solid with 125 mg in 77% yield; ^{1}H NMR (400 MHz, $CDCl_3$) δ ppm 7.81 (d, *J* = 2.74 Hz, 1H), 7.77 (d, *J* = 7.43 Hz, 1H), 7.66 (s, 1H), 7.38 - 7.47 (m, 2H), 7.30-7.36 (m, 1H), 7.21 (s, 1H), 6.95 (d, *J* = 8.61 Hz, 1H), 3.90 (s, 3H); LCMS (ESI): found $[M + Na]^+$, 364.2.

General procedure for compounds 10(a–c): Method E—Under nitrogen atmosphere, anhydrous THF (3 mL) was added to a flask containing **9a** (0.130 g, 0.38 mmol) and the mixture was stirred in an ice/brine bath for 20 min, then 4-methylmorpholine (0.04 mL, 0.38 mmol) and isopropyl chloroformate (1.0 M in THF, 0.38 mL) were added and the solution was stirred an additional 10 min. Anhydrous DMF (1.5 mL) containing methyl 4-aminobenzoate (0.057 g, 0.38 mmol) was added and the mixture was stirred in an ice/brine bath for 45 min, then removed and allowed to warm to RT while being stirred over another 2 h. The mixture was heated to 50°C overnight, then cooled and concentrated in vacuo. Excess water was added and the mixture was extracted with EtOAc (2×5mL), combined dried ethyl acetate dried over anhydrous Na_2SO_4, and concentrated in vacuo. The resulting residue was purified by silica gel chromatography with hexane/ethyl acetate combinations as eluent, giving rise to methyl 4-(3-((3,4-dichlorophenyl)sulfonamido)benzamido)benzoate (0.082 g) in 46% yield. MS (ESI): found $[M + H]^+$, 479.2. This material was dissolved in methanol/water (1/1 v/v) and LiOH (3.0 eq) were added and the solution was stirred until the methyl ester was fully hydrolyzed. The majority of methanol was removed in vacuo and the resulting solution pH~3 was adjusted with 3N aq. HCl and product was extracted with EtOAc (2×5mL), combined ethyl acetate washed with brine and dried over anhydrous Na_2SO_4, and concentrated in vacuo, then purified by HPLC (C18, 15*150 mm column; eluent: acetonitrile/water (0.05% TFA)), giving rise to the title compound **10a**.

4-(3-((3,4-dichlorophenyl)sulfonamido)benzamido)benzoic acid (10a):

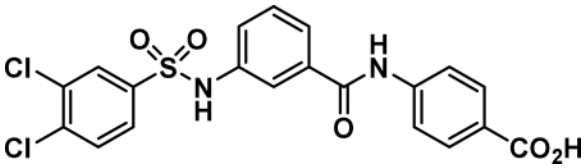

Compound synthesized as per method E, white solid with 15 mg in 19% yield; ^{1}H NMR (400 MHz, CD_3OD) δ ppm 8.03-8.01 (m, 1 H), 8.01-7.98 (m, 1 H), 7.88 (d, *J* = 2.0 Hz, 1 H), 7.79-7.77 (m, 1 H), 7.77-7.74 (m, 1 H), 7-67-7.63 (m, 2 H), 7-62-7.60 (m, 2 H), 7-57-7.53 (m, 2 H), 7.41-7.36 (m, 1 H), 7.36-7.31 (m, 1 H); LCMS (ESI): found $[M + Na]^+$, 467.1.

4-(3-((4-chlorophenyl)sulfonamido)benzamido)benzoic acid (10b):

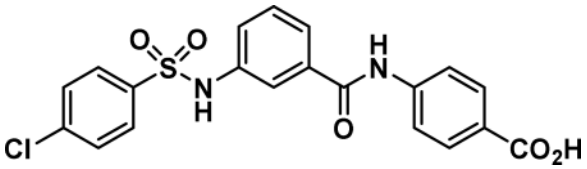

Compound synthesized as per method E, white solid with 30 g in 67% yield; ^{1}H NMR (400 MHz, CD_3OD) δ ppm 8.036-7.97 (m, 2 H), 7.78-7.66 (m, 6 H), 7.65-7.59 (m, 1 H), 7.57-7.52 (m, 1 H), 7.48-7.43 (m, 1H), 7.43-7.37 (m, 3 H), 7.36-7.28 (m, 3 H); LCMS (ESI): found $[M + H]^+$, 431.3.

4-(3-((3-chlorophenyl)sulfonamido)benzamido)benzoic acid (10c):

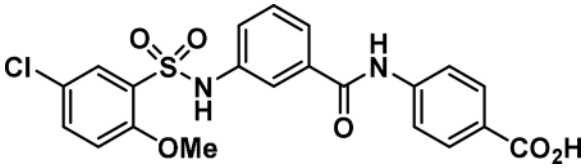

Compound synthesized as per method E, white solid with 20 mg in 61% yield; ^{1}H NMR (400 MHz, CD_3OD) δ ppm; 8.03-7.98 (m, 2 H), 7.82-7.78 (m, 2 H), 7.76 (d, *J* = 2.7 Hz, 1 H), 7-68-7.65 (m, 1 H), 7.59 (ddd, *J* = 5.6, 3.2, 1.8 Hz, 1 H), 7.49 (dd, *J* = 9.0, 2.7 Hz, 1 H), 7.39-7.35 (m, 2 H), 7.12 (d, *J* = 9.0 Hz, 1 H), 3.95 (s, 3 H); LCMS (ESI): found $[M + H]^+$, 461.2.

General procedure for compounds 14(a–b): Method F—Under nitrogen atmosphere, dry DCM (5 mL) was added to a flask containing methyl indoline-6-carboxylate **11a** (0.150 g, 0.8 mmol), then pyridine (0.28 mL, 3.5 mmol) was added. 5-chloro-2-methoxybenzenesulfonyl chloride (0.170 g, 0.7 mmol) was dissolved in dry DCM (5 mL), which was added drop wise to the flask, then the solution was stirred for 8h at RT. The mixture was poured into excess water and extracted with DCM. The organic layers were combined, washed with aqueous 1N HCl, dried with Na_2SO_4, and concentrated in vacuo. The resulting residue was purified by silica gel chromatography with hexane/ethyl acetate combinations as eluent, giving rise to methyl 1-((5-chloro-2-methoxyphenyl)sulfonyl)indoline-6-carboxylate **13a** (0.159 g) in 60% yield. MS (ESI):

found $[M + H]^+$, 382.2. This material was dissolved in methanol/water (1/1 v/v) and three equivalents of LiOH were added and the solution was stirred until the methyl ester was fully hydrolyzed. The majority of methanol was removed in vacuo and the resulting solution was extracted with EtOAc, dried with Na_2SO_4, and concentrated in vacuo, giving rise to **14a**.

1-((5-chloro-2-methoxyphenyl)sulfonyl)indoline-6-carboxylic acid (14a):

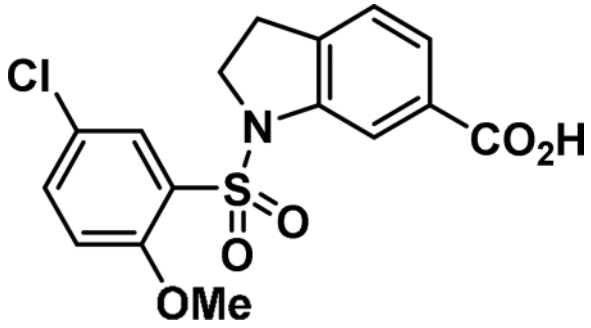

Compound synthesized as per method F, white solid with 124 mg in 81%; ^{1}H NMR (400 MHz, $CDCl_3$) δ ppm 8.07-8.04 (m, 1H), 8.01 (s, 1H), 7.68 (d, *J* = 7.83 Hz, 1H), 7.47-7.42 (m, 1H), 7.18 (d, *J* = 7.83 Hz, 1H), 6.85 (d, *J* = 8.61 Hz, 1H), 4.11 (t, *J* = 8.61 Hz, 2H), 3.63 (s, 3H), 3.10 (t, *J* = 8.61 Hz, 2H); LCMS (ESI): found $[M + Na]^+$, 390.2.

4-(3-((5-chloro-2-methoxyphenyl)sulfonamido)benzamido)benzoic acid (14b):

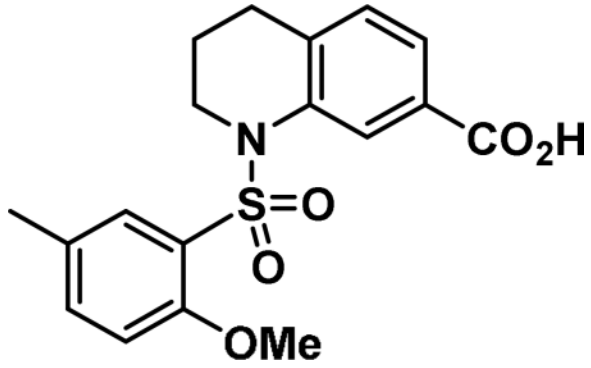

Compound synthesized as per method F, white solid with 165 mg in 83%; ^{1}H NMR (400 MHz, $CDCl_3$) δ ppm 8.10-8.04 (m, 1H), 8.02 (s, 1H), 7.70 (d, *J* = 7.81 Hz, 1H), 7.49-7.45 (m, 1H), 7.20 (d, *J* = 7.84 Hz, 1H), 6.85 (d, *J* = 8.62 Hz, 1H), 4.11 (t, *J* = 8.61 Hz, 2H), 3.63 (s, 3H), 3.10 (t, *J* = 8.61 Hz, 2H), 2.38 (s, 3H), 2.00-1.96 (m, 2H); LCMS (ESI): found $[M + Na]^+$, 461.2.

General procedure for compounds 17(a–b): Method G—Under nitrogen atmosphere, anhydrous THF (3 mL) was added to a flask containing **14a** (0.110 g, 0.30 mmol) and the mixture was stirred in an ice/brine bath for 20 min, then 4-methylmorpholine (0.03 mL, 0.30 mmol) and isopropyl chloroformate (1.0 M in THF, 0.30 mL) were added to the and the solution was stirred an additional 10 min. Anhydrous DMF (1 mL) containing methyl 4-aminobenzoate (0.045 g, 0.30 mmol) was added and the mixture was stirred in an ice/brine bath for 45 min., then removed and allowed to warm to RT while being stirred over

another 30 min. The mixture was heated to 60 °C for 4 h, then cooled and concentrated in vacuo. Excess water was added and extracted with ethyl acetate (10 mL), dried over anhydrous Na_2SO_4, and concentrated in vacuo. The resulting residue was purified by silica gel chromatography with hexane/ethyl acetate combinations as eluent, giving rise to methyl 4-(1-((5-chloro-2-methoxyphenyl)sulfonyl)indoline-6-carboxamido)benzoate **16a** (0.060 g) in 40% yield. This material was dissolved in methanol/water (1/1 v/v) and three equivalents of LiOH were added and the solution was stirred until the methyl ester was fully hydrolyzed. The majority of methanol was removed in vacuo and the resulting solution was extracted with EtOAc, dried with Na_2SO_4, and concentrated in vacuo, then purified by silica gel chromatography with methanol/dichloromethane combinations as eluent, giving rise to 45 mg of the title compound **17a**.

4-(1-((5-chloro-2-methoxyphenyl)sulfonyl)indoline-6-carboxamido)benzoic acid (17a):

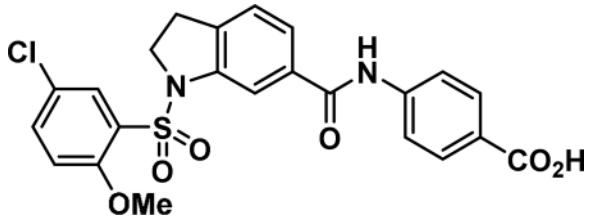

Compound synthesized as per method G, white solid with 45 mg in 77% yield; ^{1}H NMR (400 MHz, DMSO-d_6) δ ppm 12.76 (br. s., 1 H), 10.49 (s, 1 H), 7.95-7.89 (m, 3 H), 7.89-7.85 (m, 1 H), 7.73 (s, 1 H), 7.69 (dd, J = 9.0,2.7 Hz, 1 H), 7.62 (dd, J = 7.8, 1.6 Hz, 1 H), 7.36 (d, J = 7.8 Hz, 1 H), 7.21 (d, J = 9.0 Hz, 1 H), 4.10 (t, J = 8.6 Hz, 2 H), 3.66 (s, 3 H), 3.19-3.08 (m, 2H); LCMS (ESI): found $[M + H]^+$, 487.3.

4-(1-((2-methoxy-6-methylphenyl)sulfonyl)-1,2,3,4-tetrahydroquinoline-7-carboxamido)benzoic acid (17b):

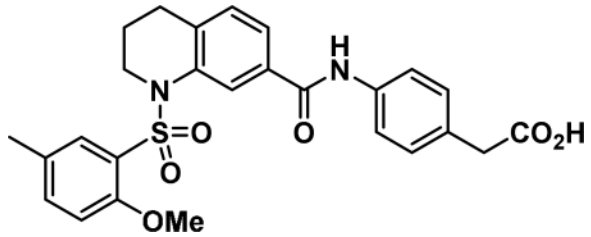

Compound synthesized as per method G, white solid with 69 mg in 82% yield; ^{1}H NMR (400 MHz, DMSO-d_6) δ ppm 10.12 (s, 1 H), 8.02 (s, 1 H), 7.71 (s, 1 H), 7.67 (d, J = 8.6 Hz, 2 H), 7.62-7.56 (m, 1 H), 7.42 (d, J = 6.7 Hz, 1H), 7.27-7.17 (m, 3 H), 7.05 (d, J = 8.6 Hz, 1 H), 3.76 (dd, J = 6.5, 4.9 Hz, 2 H), 3.55 (s, 3 H), 3.53 (s, 2 H), 2.73 (t, J = 6.5 Hz, 2 H), 2.29 (s, 3 H), 1.77-1.68 (m, 2 H); LCMS (ESI): found $[M + H]^+$, 495.4.

General procedure for compounds 23(a–c) and 24(a–c): Method H—Aryl isocyanate **22a** (1.48 mmol) was added into a solution of methyl 4-(3-aminobenzamido)benzoate **21a**[46] (0.74 mmol)in DCM (20 mL) and the solution was stirred at room temperature and product slowly get precipitated from the solution, continued stirring

for 24h. Filleted the product and washed with DCM (5mL) and pure compounds **23(a–c)** were isolated.

50% aq. NaOH solution (2 mL) was added into a solution of compounds **23a** (100 mg, 0.23 mmol) in methanol (10 mL) and stir the solution at room temperature for 24h. Progress of the reaction monitored by TLC and upon completion of the reaction, neutralized the reaction solution with 3N aq. HCl under ice bath cooling and evaporated the solvent under reduced pressure. Diluted the crude mass with water (10 mL) and acidified the solution (pH ~ 2) by con. HCl under ice bath cooling, extracted product with Ethyl acetate (3×10mL) and washed the combined organic layer with brine (10mL). Dried the Ethyl acetate layer over anhydrous Na_2SO_4 and evaporated the solvent under reduced pressure and pure compounds **24a**.

methyl 4-(3-(3-(4-(dimethylamino)phenyl)ureido)benzamido)benzoate (23a):

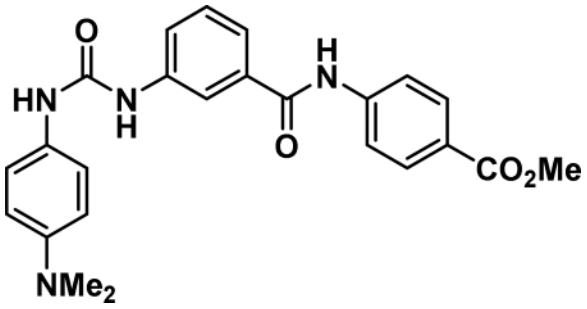

Compound synthesized as per method H, off-white solid with 90 mg in 56% yield; ^{1}H NMR (400 MHz, DMSO-d_6) δ ppm 10.56 (s, 1 H), 8.75 (s, 1 H), 8.35 (s, 1 H), 7.95 (br. s., 5 H), 7.67 (d, J = 8.2 Hz, 1 H), 7.53 (d, J = 7.4 Hz, 1 H),7.43 (t, J = 7.8 Hz, 1 H), 7.28 (s, 2 H), 6.70 (d, J = 9.0 Hz, 2 H), 3.84 (s, 3 H), 2.83 (s, 6 H);LCMS (ESI): found $[M + H]^+$, 433.3.

methyl 4-(3-(3-(4-nitrophenyl)ureido)benzamido)benzoate (23b):

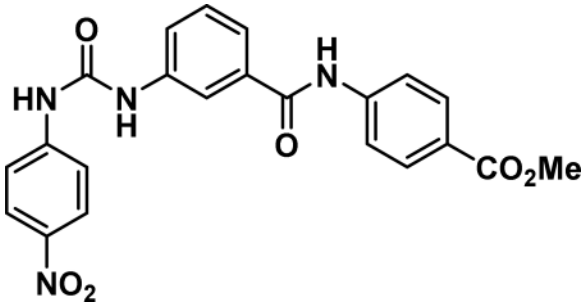

Compound synthesized as per method H, off-white solid with 200 mg in 84% yield; ^{1}H NMR (400 MHz, DMSO-d_6) δ ppm 10.59 (s, 1 H), 9.50 (s, 1 H), 9.16 (s, 1 H), 8.20 (d, J = 9.0 Hz, 2 H), 8.03 (s, 1 H), 7.90-8.00 (m, 5 H), 7.72 (d, J = 9.0 Hz, 3 H), 7.62 (d, J = 7.8 Hz, 1 H), 7.49 (t, J = 8.0 Hz, 1 H), 3.84 (s, 3 H); LCMS (ESI): found $[M + H]^+$, 435.3.

methyl 4-(3-(3-(3,4-dichlorophenyl)ureido)benzamido)benzoate (AM1079-23c):

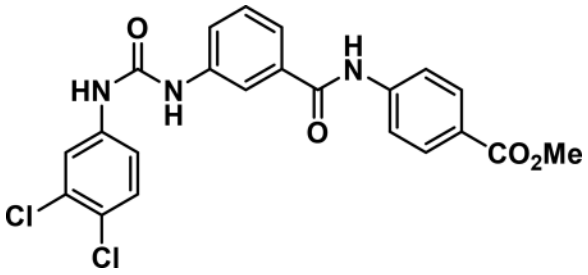

Compound synthesized as per method H, off-white solid with 120 mg in 35% yield; ^{1}H NMR (400 MHz, DMSO-d_6) δ ppm 10.58 (s, 1 H), 9.07 (s, 2 H), 8.03-7.86 (m, 7 H), 7.69 (d, J = 7.8 Hz, 1 H), 7.59 (d, J = 7.8 Hz, 1 H), 7.53 (d, J = 8.6 Hz, 1 H), 7.47 (t, J = 7.8 Hz, 1 H), 7.36 (d, J = 9.0 Hz, 1 H), 3.84 (s, 3 H); LCMS (ESI): found [M + H]$^+$, 459.3.

4-(3-(3-(4-(dimethylamino)phenyl)ureido)benzamido)benzoic acid (24a):

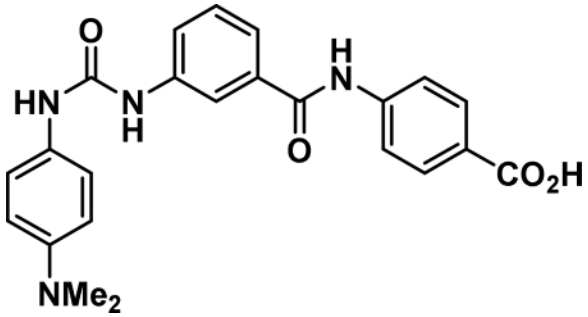

Compound synthesized as per method H, yellow solid with 10 mg in 50% yield; ^{1}H NMR (400 MHz, CD_3OD) δ ppm 8.07-7.99 (m, 3 H), 7.85 (d, J = 8.6 Hz, 2 H), 7.68-7.58 (m, 5 H), 7.50-7.44 (m, 1 H), 7.39 (br. s., 1H), 3.20 (br. s., 6 H); LCMS (ESI): found [M + H]$^+$, 419.3.

4-(3-(3-(4-nitrophenyl)ureido)benzamido) benzoic acid (24b):

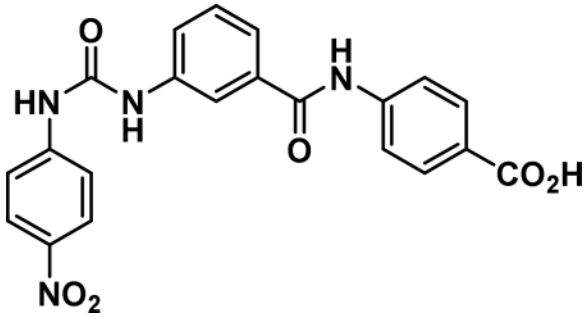

Compound synthesized as per method H, white solid with 10 mg in 50% yield; ^{1}H NMR (400 MHz, CD_3OD) δ ppm 8.22 (m, J = 9.4 Hz, 2 H), 8.06-8.00 (m, 3 H), 7.85 (m, J = 8.6 Hz, 2 H), 7.74-7.68 (m, 4 H), 7.63 (d, J = 7.8 Hz, 1 H), 7.49 (t, J = 7.8 Hz, 1 H); LCMS (ESI): found [M + H]$^+$, 421.3.

4-(3-(3-(3,4-dichlorophenyl)ureido)benzamido) benzoic acid (24c):

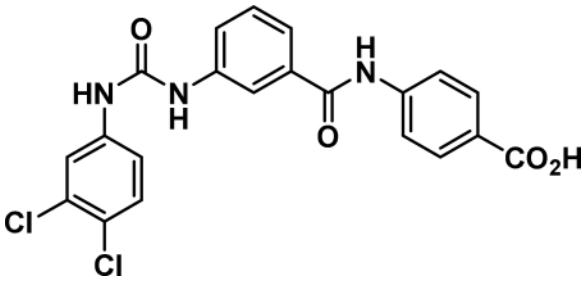

Compound synthesized as per method H, white solid with 61 mg in 77% yield; ^{1}H NMR (400 MHz, CD_3OD) δ ppm 10.54 (s, 1 H), 9.08 (d, *J* = 4.7 Hz, 2 H), 8.06-7.85 (m, 6 H), 7.69 (d, *J* = 7.8 Hz, 1 H), 7.59 (d, *J* = 7.4 Hz, 1 H), 7.53 (d, *J* = 8.6 Hz, 1 H), 7.50-7.42 (m, 1 H), 7.36 (d, *J* = 9.0 Hz, 1 H); LCMS (ESI): found $[M + Na]^+$, 445.3.

Supplementary Material

Refer to Web version on PubMed Central for supplementary material.

Acknowledgments

We thank Qi Wang for her technical assistance related to clustering compounds and identifying representatives for screening. This work was supported by National Institute of Allergy and Infectious Diseases (NIAID) grant AI081803 to M.M. The study was also partly supported by NIAID grant AI056189 to R.V.A.

ABBREVIATIONS USED

CPT	carnitine palmitoyltransferase
MDA	mass drug administration
EC	Enzyme Commission number
PHX	perhexiline
STH	soil transmitted helminth
DMSO	dimethyl sylfoxide
SAR	structure activity relationships
PDB	Protein Databank
EDCI/EDC	1-Ethyl-3-(3-dimethylaminopropyl)carbodiimide
DIPEA	N,N-diisopropylethylamine
DMF	dimethylformamide
HPLC	high-performance liquid chromatography
LC-MS/LCMS	liquid chromatography–mass spectrometry
HEPES	4-(2-hydroxyethyl)-1-piperazineethanesulfonic acid

MMU	mean movement unit
SDS	sodium dodecyl sulfate
TFA	trifluoroacetic acid
PBS	phosphate-buffered saline
iL3	infective L3 larval stage
p.i.	post infection
NMR	nuclear magnetic resonance
TLC	thin layer chromatography
DCM	dichloromethane
DMAP	4-Dimethylaminopyridine
RT	room temperature
CDI	1,1'-Carbonyldiimidazole
HOBt	Hydroxybenzotriazole
EtOAc	Ethyl acetate

References

1. Collaborators, G. D. a. I. I. a. P. Global, regional, and national incidence, prevalence, and years lived with disability for 310 diseases and injuries, 1990–2015: a systematic analysis for the Global Burden of Disease Study 2015. Lancet. 2016; 388(10053):1545–1602. DOI: 10.1016/S0140-6736(16)31678-6 [PubMed: 27733282]
2. Whitehead AG. Plant nematode control. CAB; Wallingford, UK: 1998.
3. Mavrot F, Hertzberg H, Torgerson P. Effect of gastro-intestinal nematode infection on sheep performance: a systematic review and meta-analysis. Parasit Vectors. 2015; 8:557.doi: 10.1186/s13071-015-1164-z [PubMed: 26496893]
4. Molyneux DH, Savioli L, Engels D. Neglected tropical diseases: progress towards addressing the chronic pandemic. Lancet. 2017; 389(10066):312–325. DOI: 10.1016/S0140-6736(16)30171-4 [PubMed: 27639954]
5. McCarty TR, Turkeltaub JA, Hotez PJ. Global progress towards eliminating gastrointestinal helminth infections. Curr Opin Gastroenterol. 2014; 30(1):18–24. DOI: 10.1097/MOG.0000000000000025 [PubMed: 24241244]
6. Helmy H, Weil GJ, Ellethy AS, Ahmed ES, Setouhy ME, Ramzy RM. Bancroftian filariasis: effect of repeated treatment with diethylcarbamazine and albendazole on microfilaraemia, antigenaemia and antifilarial antibodies. Trans R Soc Trop Med Hyg. 2006; 100(7):656–62. DOI: 10.1016/j.trstmh.2005.08.015 [PubMed: 16414095]
7. Moulia-Pelat JP, Glaziou P, Weil GJ, Nguyen LN, Gaxotte P, Nicolas L. Combination ivermectin plus diethylcarbamazine, a new effective tool for control of lymphatic filariasis. Trop Med Parasitol. 1995; 46(1):9–12. [PubMed: 7631132]
8. Kaplan RM, Vidyashankar AN. An inconvenient truth: global worming and anthelmintic resistance. Veterinary parasitology. 2012; 186(1–2):70–8. DOI: 10.1016/j.vetpar.2011.11.048 [PubMed: 22154968]

9. Abongwa M, Marjanovic DS, Tipton JG, Zheng F, Martin RJ, Trailovic SM, Robertson AP. Monepantel is a non-competitive antagonist of nicotinic acetylcholine receptors from Ascaris suum and Oesophagostomum dentatum. Int J Parasitol Drugs Drug Resist. 2017; 8(1):36–42. DOI: 10.1016/j.ijpddr.2017.12.001 [PubMed: 29366967]
10. Buxton SK, Neveu C, Charvet CL, Robertson AP, Martin RJ. On the mode of action of emodepside: slow effects on membrane potential and voltage-activated currents in Ascaris suum. Br J Pharmacol. 2011; 164(2b):453–70. DOI: 10.1111/j.1476-5381.2011.01428.x [PubMed: 21486286]
11. Rufener L, Maser P, Roditi I, Kaminsky R. Haemonchus contortus acetylcholine receptors of the DEG-3 subfamily and their role in sensitivity to monepantel. PLoS Pathog. 2009; 5(4):e1000380.doi: 10.1371/journal.ppat.1000380 [PubMed: 19360096]
12. Taylor CM, Wang Q, Rosa BA, Huang SC-C, Powell K, Schedl T, Pearce EJ, Abubucker S, Mitreva M. Discovery of Anthelmintic Drug Targets and Drugs Using Chokepoints in Nematode Metabolic Pathways. PLoS Pathog. 2013; 9(8):e1003505.doi: 10.1371/journal.ppat.1003505 [PubMed: 23935495]
13. Tyagi R, Rosa BA, Lewis WG, Mitreva M. Pan-phylum Comparison of Nematode Metabolic Potential. PLoS Negl Trop Dis. 2015; 9(5):e0003788.doi: 10.1371/journal.pntd.0003788 [PubMed: 26000881]
14. Kim TY, Kim HU, Lee SY. Metabolite-centric approaches for the discovery of antibacterials using genome-scale metabolic networks. Metab Eng. 2010; 12(2):105–11. DOI: 10.1016/j.ymben.2009.05.004 [PubMed: 19481614]
15. Ceccarelli SM, Chomienne O, Gubler M, Arduini A. Carnitine palmitoyltransferase (CPT) modulators: a medicinal chemistry perspective on 35 years of research. J Med Chem. 2011; 54(9):3109–52. DOI: 10.1021/jm100809g [PubMed: 21504156]
16. Wagman AS, Nuss JM. Current therapies and emerging targets for the treatment of diabetes. Curr Pharm Des. 2001; 7(6):417–50. [PubMed: 11281851]
17. Winchester DE, Pepine CJ. Angina treatments and prevention of cardiac events: an appraisal of the evidence. Eur Heart J Suppl. 2015; 17(Suppl G):G10–G18. DOI: 10.1093/eurheartj/suv054 [PubMed: 26740801]
18. Klug DM, Gelb MH, Pollastri MP. Repurposing strategies for tropical disease drug discovery. Bioorg Med Chem Lett. 2016; 26(11):2569–76. DOI: 10.1016/j.bmcl.2016.03.103 [PubMed: 27080183]
19. Wang Q, Heizer E, Rosa BA, Wildman SA, Janetka JW, Mitreva M. Characterization of parasite-specific indels and their proposed relevance for selective anthelminthic drug targeting. Infect Genet Evol. 2016; 39:201–211. DOI: 10.1016/j.meegid.2016.01.025 [PubMed: 26829384]
20. Ashrafian H, Horowitz JD, Frenneaux MP. Perhexiline. Cardiovasc Drug Rev. 2007; 25(1):76–97. DOI: 10.1111/j.1527-3466.2007.00006.x [PubMed: 17445089]
21. Maggiora G, Vogt M, Stumpfe D, Bajorath J. Molecular similarity in medicinal chemistry. J Med Chem. 2014; 57(8):3186–204. DOI: 10.1021/jm401411z [PubMed: 24151987]
22. Lipinski CA. Lead- and drug-like compounds: the rule-of-five revolution. Drug Discov Today Technol. 2004; 1(4):337–41. DOI: 10.1016/j.ddtec.2004.11.007 [PubMed: 24981612]
23. Labonté R, Baum F, Sanders D. Poverty, justice, and health. Oxford Textbook of Global Public Health. 2015; 89
24. Blaxter ML, De Ley P, Garey JR, Liu LX, Scheldeman P, Vierstraete A, Vanfleteren JR, Mackey LY, Dorris M, Frisse LM, Vida JT, Thomas WK. A molecular evolutionary framework for the phylum Nematoda. Nature. 1998; 392(6671):71–5. DOI: 10.1038/32160 [PubMed: 9510248]
25. Yin X, Dwyer J, Langley SR, Mayr U, Xing Q, Drozdov I, Nabeebaccus A, Shah AM, Madhu B, Griffiths J, Edwards LM, Mayr M. Effects of perhexiline-induced fuel switch on the cardiac proteome and metabolome. J Mol Cell Cardiol. 2013; 55:27–30. DOI: 10.1016/j.yjmcc.2012.12.014 [PubMed: 23277191]
26. Thupari JN, Landree LE, Ronnett GV, Kuhajda FP. C75 increases peripheral energy utilization and fatty acid oxidation in diet-induced obesity. Proc Natl Acad Sci U S A. 2002; 99(14):9498–502. DOI: 10.1073/pnas.132128899 [PubMed: 12060712]

27. Bentebibel A, Sebastián D, Herrero L, López-Viñas E, Serra D, Asins G, Gómez-Puertas P, Hegardt FG. Novel effect of C75 on carnitine palmitoyltransferase I activity and palmitate oxidation. Biochemistry. 2006; 45(14):4339–50. DOI: 10.1021/bi052186q [PubMed: 16584169]
28. Tseng CC, Noordali H, Sani M, Madhani M, Grant DM, Frenneaux MP, Zanda M, Greig IR. Development of Fluorinated Analogues of Perhexiline with Improved Pharmacokinetic Properties and Retained Efficacy. J Med Chem. 2017; 60(7):2780–2789. DOI: 10.1021/acs.jmedchem.6b01592 [PubMed: 28277663]
29. Gu L, Liu H, Gu X, Boots C, Moley KH, Wang Q. Metabolic control of oocyte development: linking maternal nutrition and reproductive outcomes. Cell Mol Life Sci. 2015; 72(2):251–71. DOI: 10.1007/s00018-014-1739-4 [PubMed: 25280482]
30. Pearce EJ, Huang SC. The metabolic control of schistosome egg production. Cell Microbiol. 2015; 17(6):796–801. DOI: 10.1111/cmi.12444 [PubMed: 25850569]
31. Rosa BA, Jasmer DP, Mitreva M. Genome-wide tissue-specific gene expression, co-expression and regulation of co-expressed genes in adult nematode Ascaris suum. PLoS Negl Trop Dis. 2014; 8(2):e2678.doi: 10.1371/journal.pntd.0002678 [PubMed: 24516681]
32. Blaxter ML. Nematoda: genes, genomes and the evolution of parasitism. Adv Parasitol. 2003; 54:101–95. [PubMed: 14711085]
33. Adoutte A, Balavoine G, Lartillot N, de Rosa R. Animal evolution. The end of the intermediate taxa? Trends Genet. 1999; 15(3):104–8. [PubMed: 10203807]
34. Soukhathammavong PA, Sayasone S, Phongluxa K, Xayaseng V, Utzinger J, Vounatsou P, Hatz C, Akkhavong K, Keiser J, Odermatt P. Low efficacy of single-dose albendazole and mebendazole against hookworm and effect on concomitant helminth infection in Lao PDR. PLoS Negl Trop Dis. 2012; 6(1):e1417.doi: 10.1371/journal.pntd.0001417 [PubMed: 22235353]
35. Hu Y, Ellis BL, Yiu YY, Miller MM, Urban JF, Shi LZ, Aroian RV. An extensive comparison of the effect of anthelmintic classes on diverse nematodes. PLoS One. 2013; 8(7):e70702.doi: 10.1371/journal.pone.0070702 [PubMed: 23869246]
36. Fischer S, Brunk BP, Chen F, Gao X, Harb OS, Iodice JB, Shanmugam D, Roos DS, Stoeckert CJ. Using OrthoMCL to assign proteins to OrthoMCL-DB groups or to cluster proteomes into new ortholog groups. Curr Protoc Bioinformatics. 2011; (Unit 6.12):1–19. Chapter 6. DOI: 10.1002/0471250953.bi0612s35
37. Martin J, Rosa BA, Ozersky P, Hallsworth-Pepin K, Zhang X, Bhonagiri-Palsikar V, Tyagi R, Wang Q, Choi YJ, Gao X, McNulty SN, Brindley PJ, Mitreva M. Helminth.net: expansions to Nematode.net and an introduction to Trematode.net. Nucleic Acids Res. 2015; 43(Database issue):D698–706. DOI: 10.1093/nar/gku1128 [PubMed: 25392426]
38. Guha R, Howard MT, Hutchison GR, Murray-Rust P, Rzepa H, Steinbeck C, Wegner J, Willighagen EL. The Blue Obelisk-interoperability in chemical informatics. J Chem Inf Model. 2006; 46(3):991–8. DOI: 10.1021/ci050400b [PubMed: 16711717]
39. Irwin JJ, Shoichet BK. ZINC--a free database of commercially available compounds for virtual screening. J Chem Inf Model. 2005; 45(1):177–82. DOI: 10.1021/ci049714+ [PubMed: 15667143]
40. Rufer AC, Thoma R, Benz J, Stihle M, Gsell B, De Roo E, Banner DW, Mueller F, Chomienne O, Hennig M. The crystal structure of carnitine palmitoyltransferase 2 and implications for diabetes treatment. Structure. 2006; 14(4):713–23. DOI: 10.1016/j.str.2006.01.008 [PubMed: 16615913]
41. Conti R, Mannucci E, Pessotto P, Tassoni E, Carminati P, Giannessi F, Arduini A. Selective reversible inhibition of liver carnitine palmitoyl-transferase 1 by teglicar reduces gluconeogenesis and improves glucose homeostasis. Diabetes. 2011; 60(2):644–51. DOI: 10.2337/db10-0346 [PubMed: 21270274]
42. Case DA, Darden T, Cheatham T, Simmerling CL, Wang J, Duke RE, Luo R, Crowley M, Walker RC, Zhang W. Amber 10. University of California; 2008.
43. Marcellino C, Gut J, Lim KC, Singh R, McKerrow J, Sakanari J. WormAssay: a novel computer application for whole-plate motion-based screening of macroscopic parasites. PLoS Negl Trop Dis. 2012; 6(1):e1494.doi: 10.1371/journal.pntd.0001494 [PubMed: 22303493]
44. Hu Y, Miller MM, Derman AI, Ellis BL, Monnerat RG, Pogliano J, Aroian RV. Bacillus subtilis strain engineered for treatment of soil-transmitted helminth diseases. Appl Environ Microbiol. 2013; 79(18):5527–32. DOI: 10.1128/AEM.01854-13 [PubMed: 23835175]

45. a) Johns BA, Kawasuji T, Taishi T, Taoda Y. Polycyclic carbamoylpyridone derivative having HIV integrase inhibitory activity and their preparation. PCT Int. Appl. WO. 2006116764. 2006. b) Andjekovic M, Ceccarelli SM, Chomienne O, Mattei P. preparation of phenoxyacetylpiperidinylthiaziles as liver carnitine palmytoyl transferase (L-CPT1) inhibitors. U.S. Pat. Appl. Publ. US. 20080300279. 2008.

46. Chen Y, Wen D, Huang Z, Huang M, Luo Y, Liu B, Lu H, Wu Y, Peng Y, Zhang J. 2-(4-Chlorophenyl)-2-oxoethyl 4-benzamidobenzoate derivatives, a novel class of SENP1 inhibitors: Virtual screening, synthesis and biological evaluation. Bioorganic & Medicinal Chemistry Letters. 2012; 22(22):6867–6870. [PubMed: 23044371]

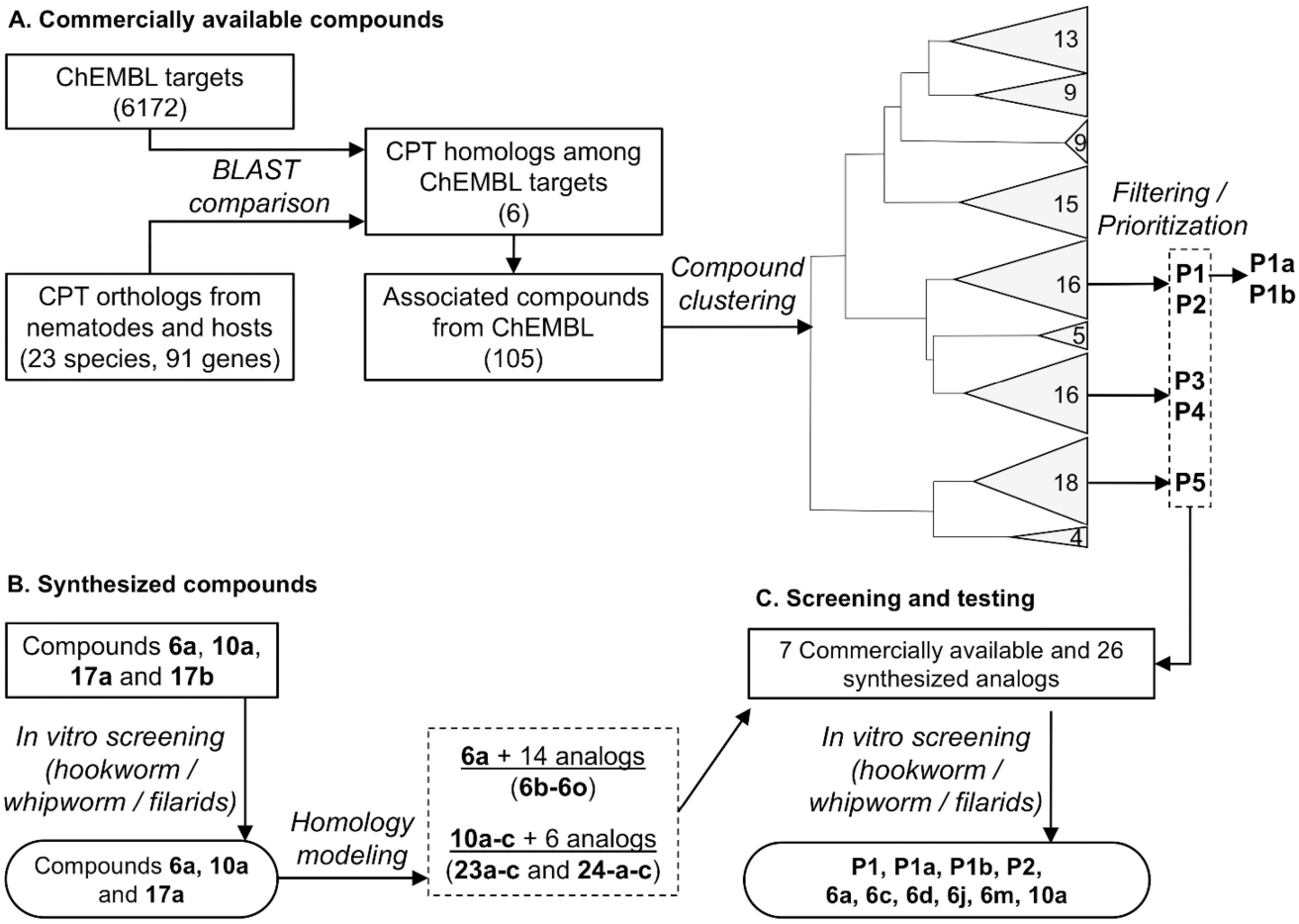

Figure 1.

Overall workflow. (A) Identification of publicly available CPT-modulators: CPT orthologs in 23 species were identified and used to find CPT homologs in ChEMBL's target database. The 105 compounds targeting these CPT homologs in the ChEMBL database were grouped into nine clusters based on their structure and five representatives were prioritized for screening after filtering for drug-likeness, commercial availability and cost. (B) Synthesizing known mammalian CPT-modulators. Four known CPT inhibitor compounds were synthesized and used in *in vitro* screening. Two of these were found to be deleterious to the worms, and were used for docking studies. Based on the docking results 22 analogs were synthesized and used for *in vitro* screening. (C) *in vitro* screening was accomplished for a total of 33 compounds in adult stage of multiple parasitic nematode species, of those 10 were hits in both intestinal and filarial nematodes.

A

Group	S. No.	Compound	Motility Index: Tested molarity (μM)*	*N. brasiliensis* 48 hrs	*H. polygyrus* 72 hrs	*A. ceylanicum* 24hrs	*T. suis* 48 hrs	Motility inhibition (%): *B. pahangi* (100 μM)* 72 hrs
Commercially available inhibitors	P1	Perhexiline malate salt	203	**0.00**	**0.00**	**0.00**	**0.00**	**100**
	P2	(C75) 4-Methylene-2-octyl-5-oxotetrahydrofuran-3-carboxylic acid	315	2.37	1.83	1.90	**0.00**	**95**
	P3	sodium 2-(4-hydroxyphenyl)-2-oxoacetate	339	2.55	2.17	2.30	2.88	10
	P4	1-[(2,3,4-trimethoxyphenyl) methyl]piperazine dihydrochloride	236	**1.01**	2.71	2.30	3.00	0
	P5	Methyl 2-methylglycidate	344	2.57	1.29	2.80	**0.00**	2
Synthesized known mamalian CPT inhibitors	6a	$C_{21}H_{21}N_3O_2S$	211	**0.10**	1.50	2.00	**0.00**	**96**
	10a	$C_{20}H_{14}Cl_2N_2O_5S$	172	**0.69**	1.83	2.00	3.00	**100**
	17a	$C_{23}H_{19}ClN_2O_6S$	164	2.51	2.46	**1.00**	2.90	30
	17b	$C_{26}H_{26}N_2O_6S$	162	2.10	2.67	2.00	3.00	0

Motility Index code 3 High motility 2 Motile 1 Motile only when touched 0 No motility at all

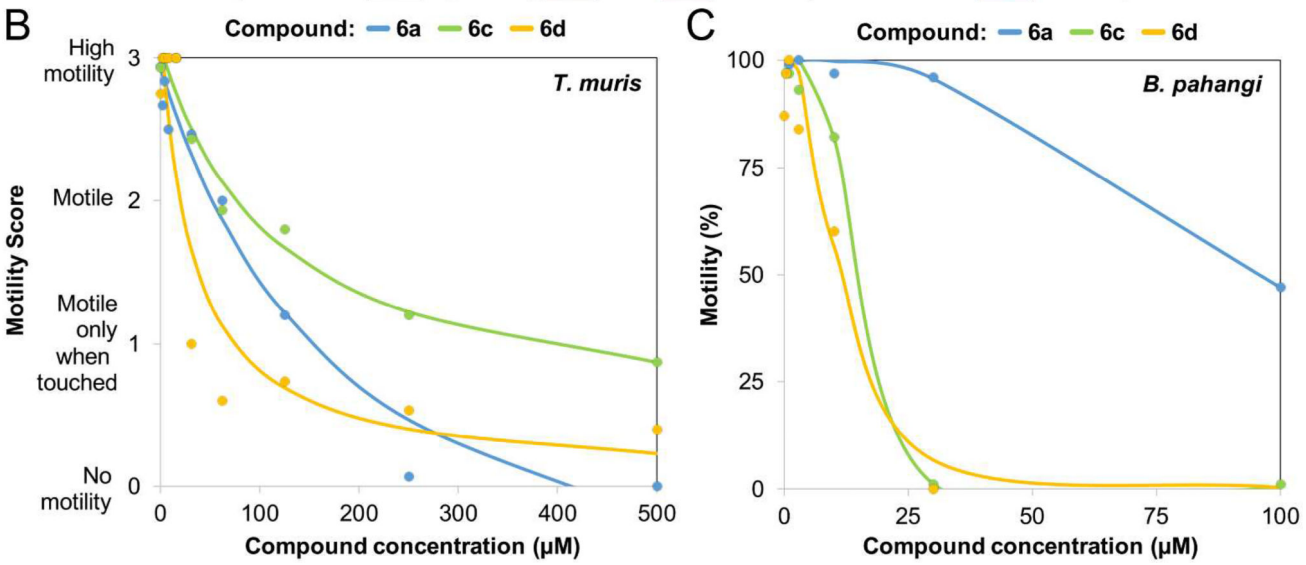

Figure 2.

I*n vitro* screening in intestinal and filarial nematodes. (A) Compounds screened to identify their pan-phylum potential based on motility inhibition. For complete set of results and details on the molecular weight and tested concentrations see Table S4. Dose response assay data for **6a** and its analogs **6c** and **6d** from *in vitro* screening of whipworm (B) and filarial nematode (C). This is a subset compiled from the full dataset to illustrate the most striking results.

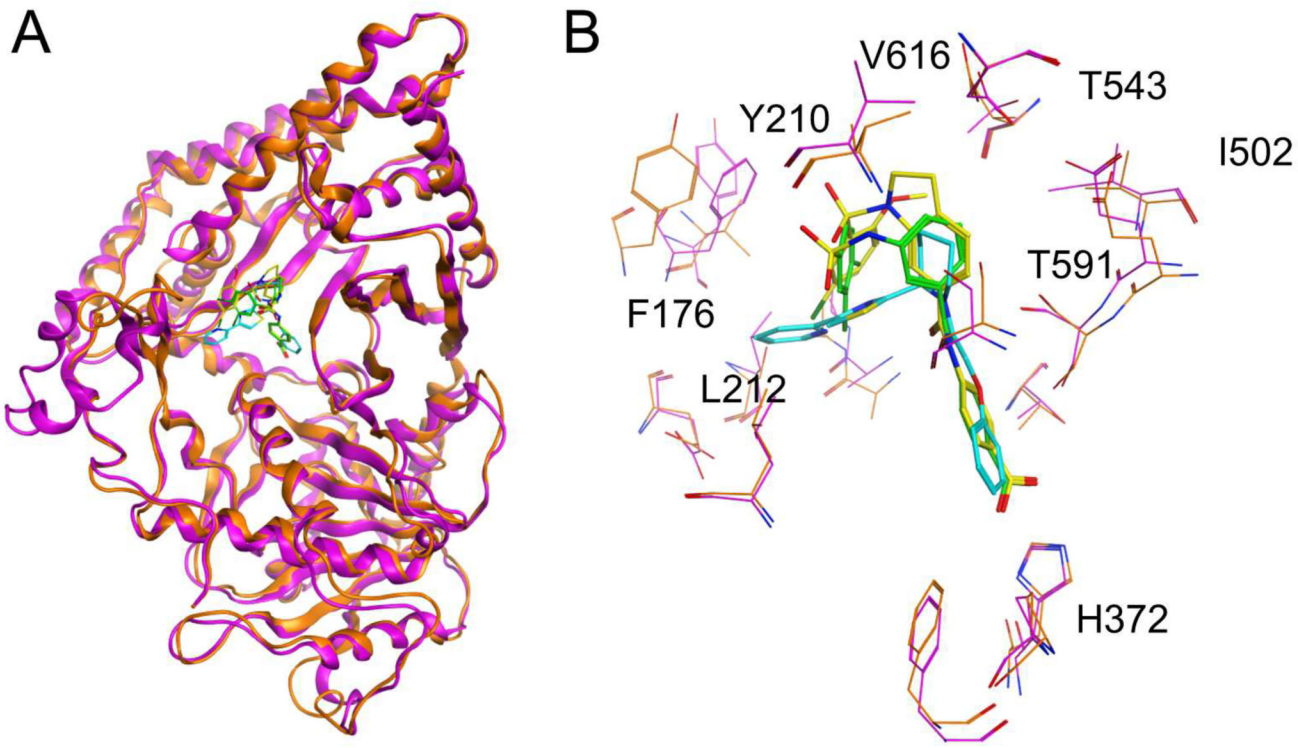

Figure 3.

(A) Molecular docking of inhibitors bound to *T. muris* CPT2 (orange) based on rat CPT2 2FW3 (magenta). (B) Overlay of **6a** (cyan), **10a** (green) and **17a** (yellow). Residues of CPT2 homology model in *T. muris* are in orange and rat CPT2 is in magenta. Targeted differences in the CoA binding site of *T. muris* are shown as sticks. (i) Thr (rat), Val (*Tm*); (i) Phe (rat), Tyr (*Tm*); (iii) Lys (rat), Arg (*Tm*); (iv) Asn (rat), Thr (*Tm*).

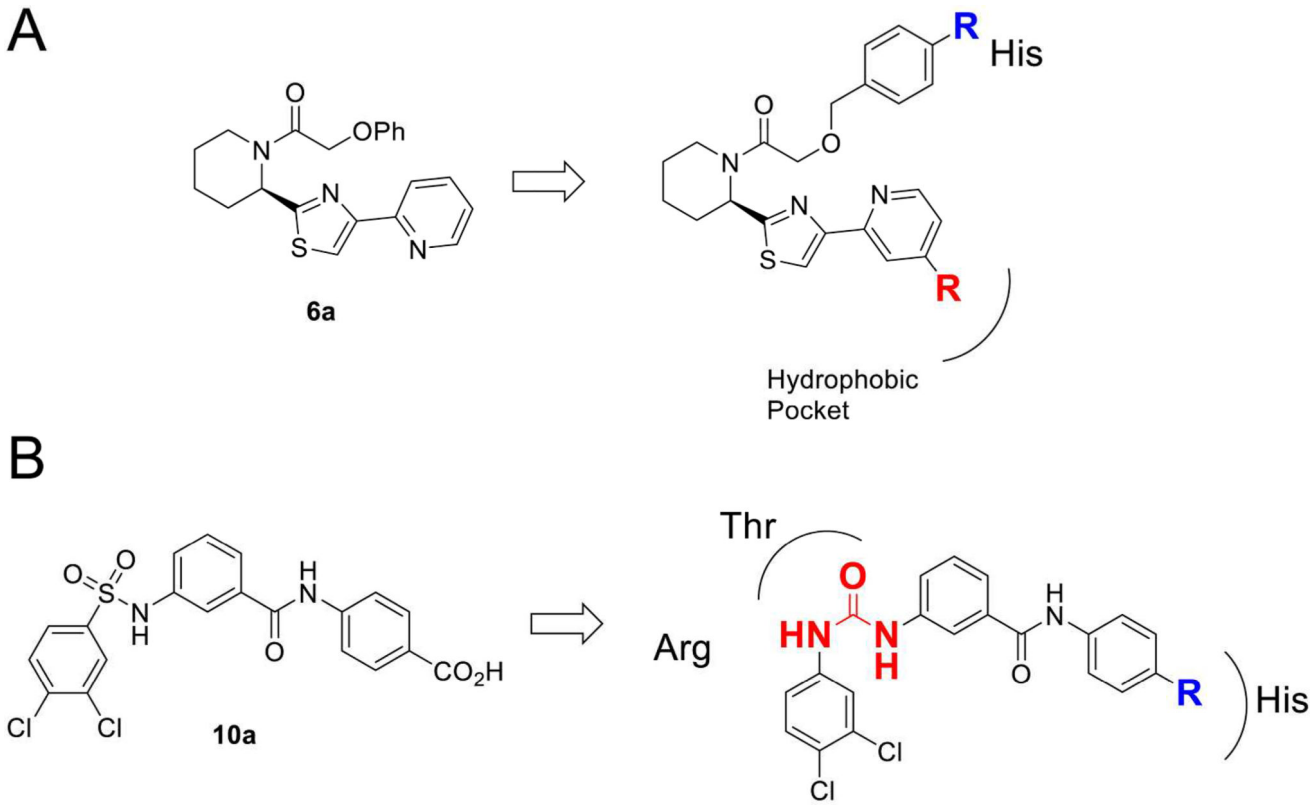

Figure 4.
Rational design chemistry plan: (A) **6a** and (B) **10a**.

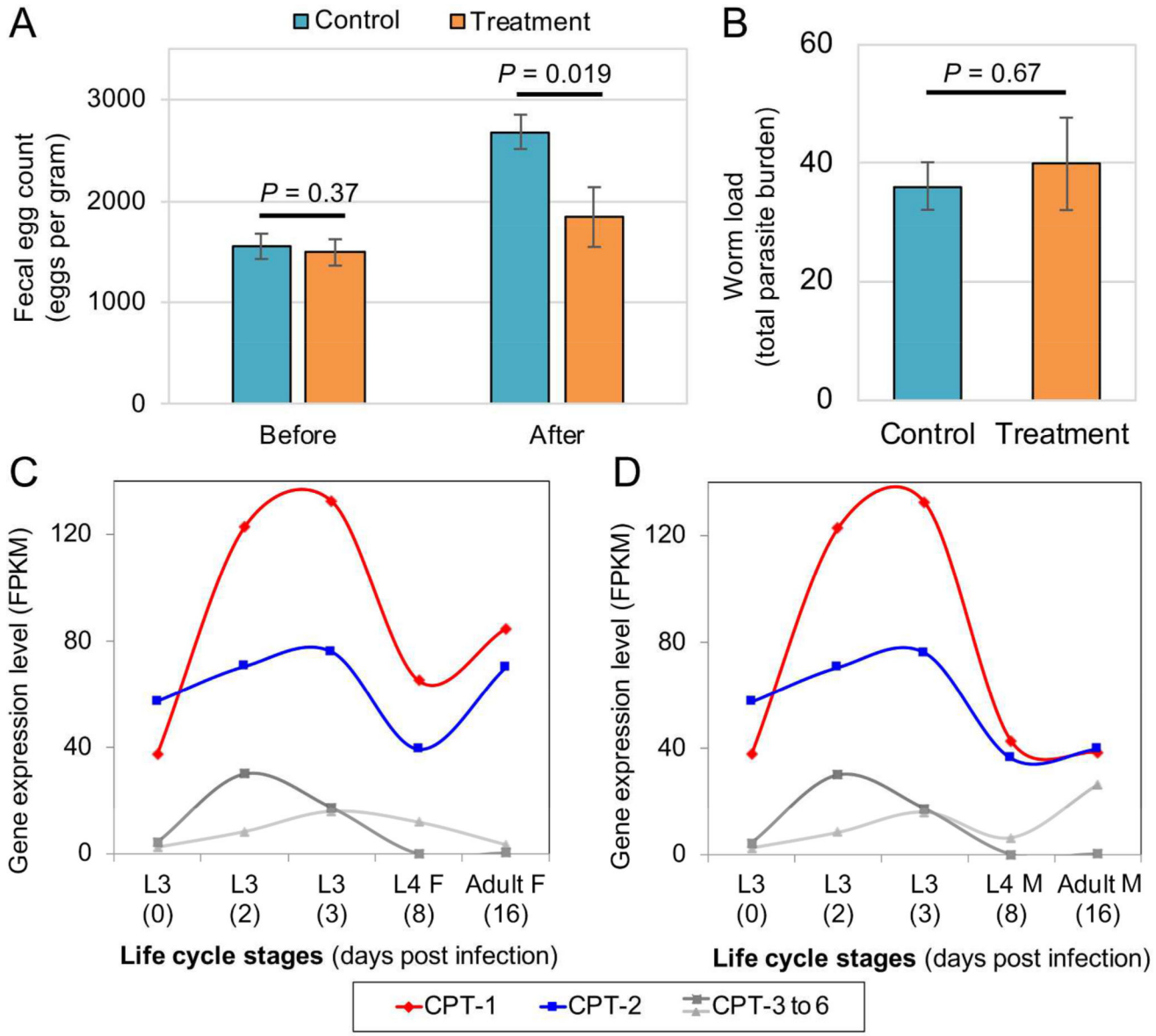

Figure 5.

Perhexiline reduces fecal egg count but not total worm load. (A) Treatment with perhexiline significantly reduced fecal egg count in Syrian hamsters infected with the hookworm *A. ceylanicum* compared with untreated control animals. (B) The fecal egg count reduction was not accompanied by a reduction of worm load, which was not statistically significant between control and treated animals. (C) and (D) RNAseq based gene expression profile over developmental stages of *A. ceylanicum* shows increased expression of CPT1/2 in adult female compared to L4 female, L4 male and adult male.

Scheme A. Synthesis of compounds **6**(**a-o**)

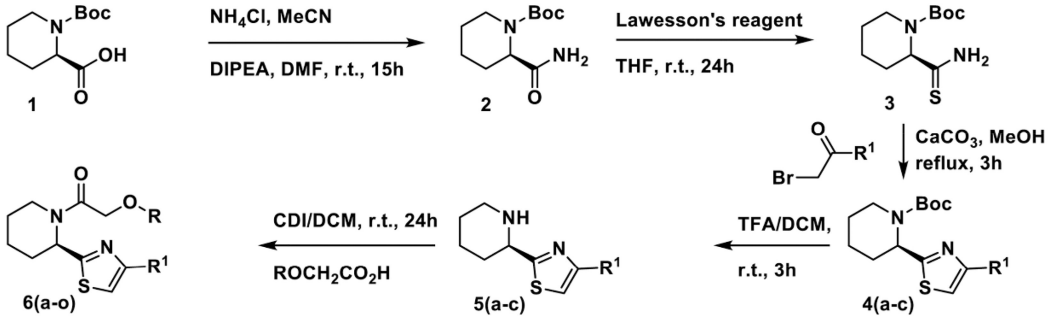

R = Ph, R^1 = pyridin-2-yl (**6a**); R = 4-biphyl, R^1 = pyridin-2-yl (**6b**); R = 1-naphthalene, R^1 = pyridin-2-yl (**6c**); R = 2-naphthalene, R^1 = pyridin-2-yl (**6d**); R = 1-phenyl-4-adamantane, R^1 = pyridin-2-yl (**6e**); R = Ph, R^1 = 4-methoxyphenyl (**6f**); R = 1-Phenyl-4-cyclohexane, R^1 = pyridin-2-yl, (**6g**); R = 1-diphenylmethane, R^1 = pyridin-2-yl (**6h**), R = 4-methyl-1,1'-biphenyl, R^1 = pyridin-2-yl (**6i**); R = 2-phenylpyridine, R^1 = pyridin-2-yl (**6j**); R = Ph, R^1 = naphthalen-2-yl (**6k**); R = Ph(4-CO_2Me), R^1 = pyridin-2-yl (**6l**); R = Ph(3-CO_2Me), R^1 = pyridin-2-yl (**6m**); R = Ph(4-CO_2H),R^1 = pyridin-2-yl (**6n**); R = Ph(3-CO_2H),R^1 = pyridin-2-yl (**6o**)

Scheme B. Synthesis of compounds **10**(**a-c**)

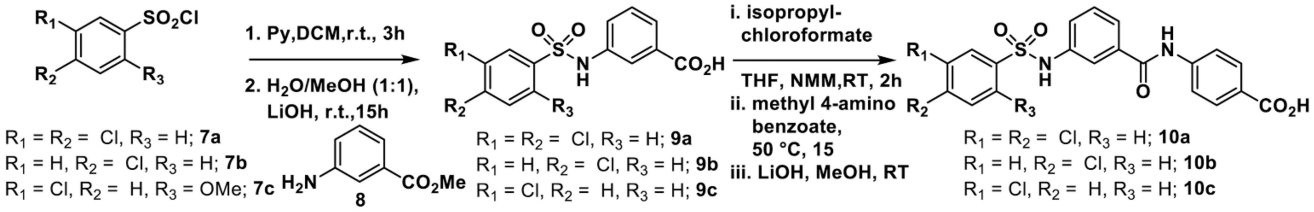

R_1 = R_2 = Cl, R_3 = H; **7a**
R_1 = H, R_2 = Cl, R_3 = H; **7b**
R_1 = Cl, R_2 = H, R_3 = OMe; **7c**

R_1 = R_2 = Cl, R_3 = H; **9a**
R_1 = H, R_2 = Cl, R_3 = H; **9b**
R_1 = Cl, R_2 = H, R_3 = H; **9c**

R_1 = R_2 = Cl, R_3 = H; **10a**
R_1 = H, R_2 = Cl, R_3 = H; **10b**
R_1 = Cl, R_2 = H, R_3 = H; **10c**

Scheme 1.

Synthesis of known mammalian small molecule CPT inhibitors and analogs. (A) Synthesis of known compound **6a** and its newly designed analogs. (B) Synthesis of known compound **10a** and its newly designed analogs.

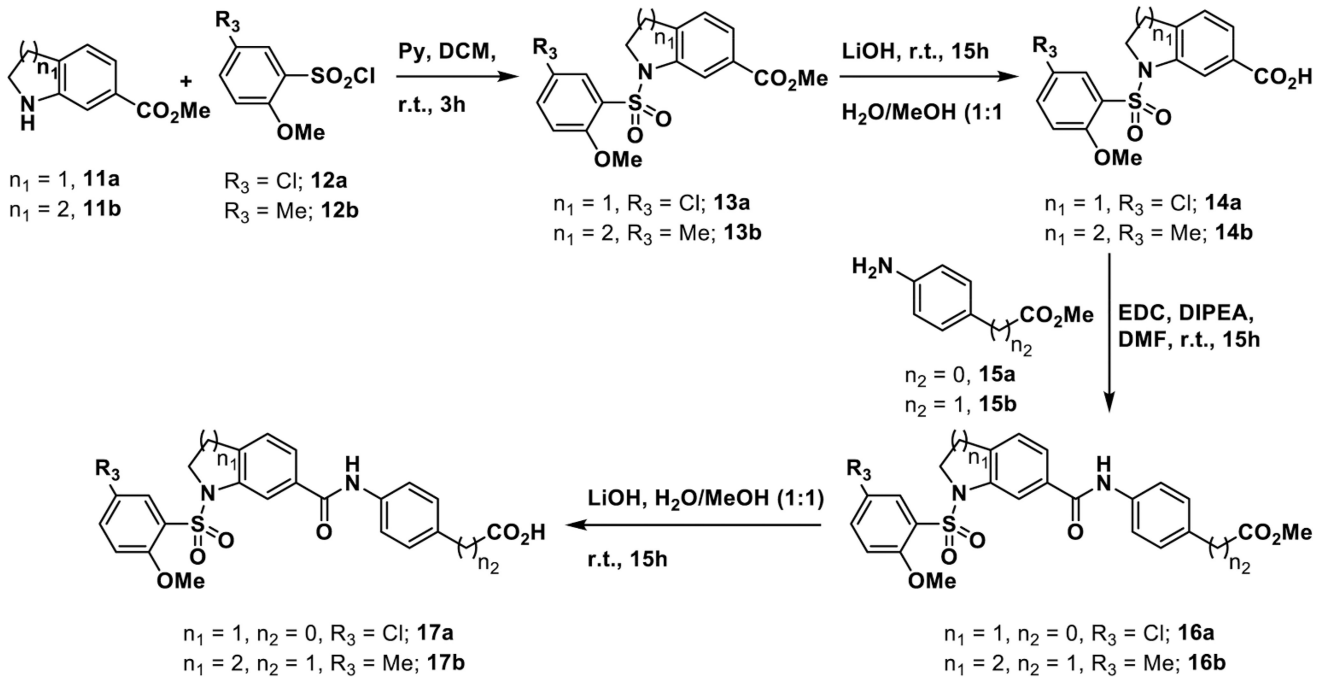

Scheme 2.

Synthesis of known CPT inhibitors **17(a–b)** as conformationally restricted sulfonamide analogs of **6a**.

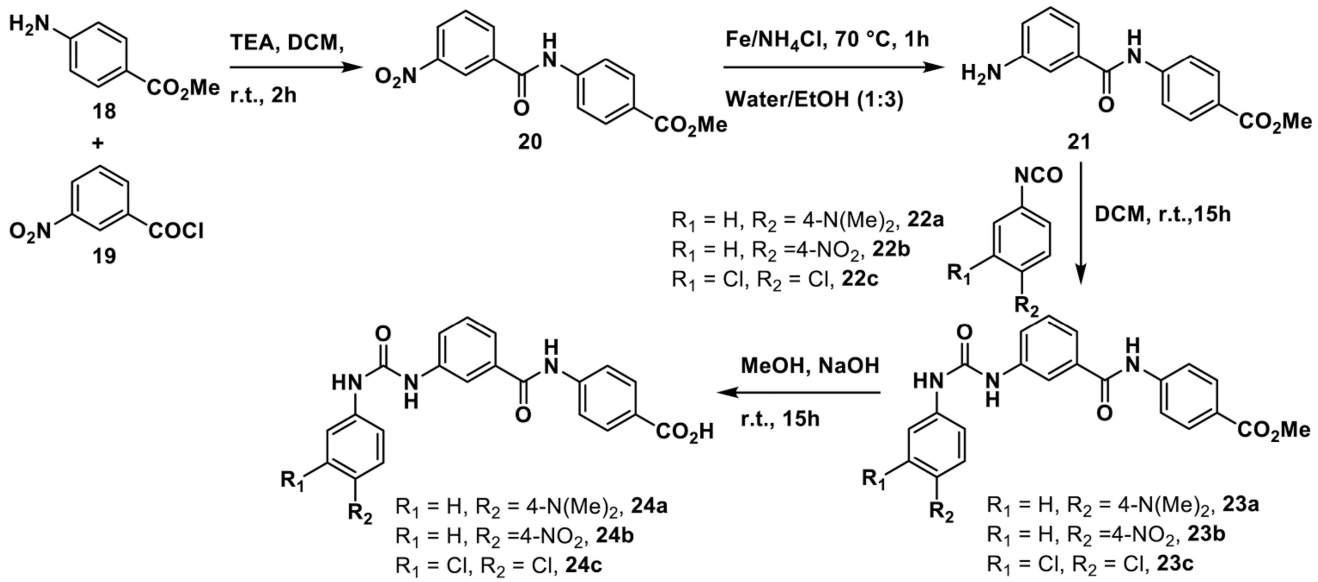

Scheme 3.

Synthesis of compounds **24(a–c)** as novel urea analogs of known CPT inhibitor **10a**.